

## *Chapter - 6*



# *Cause of Colour and Enhancement*

## 6 - COLOUR OF BERYL AND ENHANCEMENT

### 6.1 INTRODUCTION

The term colour is used to describe atleast three subtly different aspects. Firstly, it describes appearance of an object, as in *green grass*. Secondly, it describes characteristic light rays as in *grass* that efficiently reflects green hue while absorbing other wavelengths and further, it describes a class of sensation perceived in the brain. Surprisingly several preconceived ideas exists in minds of many people such as deep blue to cobalt as in cobalt glass. Deep blue may be due cobalt (synthetic blue spinel), iron (aquamarine and tourmaline), copper (azurite and turquoise), iron plus titanium (blue sapphire) or a colour centre without any transition metal impurity (Maxixe type beryl), boron (diamond), organic compound (coral), opal (diffraction and interference of light), blue aventurine quartz (due to dumortierite inclusion) Like wise the same chromophoric ion may yield different colour in various minerals. The chromium compounds can be red, green, orange, yellow, brown and even lilac depending on it position in the crystal structure (Nassau, 1983)

Only in recent times cause of colour in various substances have been understood scientifically, largely due to Dr. Kurt Nassau of Bell Laboratories, New York, USA. As many as 15 causes of colour (*Table 6.1*) have been identified by Nassau (1983). Of these causes, 4 to 15 (*Table 6.1*) pertain to minerals. For identifying the cause of colour in a material (mineral) it requires a variety of tools such as spectroscopy and chemical analysis, and often the mineral may have to be artificially irradiated and heated. A crystal may even have to be synthesised to identify the cause of colour

**Table 6.1 : Various causes of colours in minerals/gemstone (Nassau, 1983)**

Colour cause	Typical Mineral/Gemstones	Theory
1 Incandescence	Flames, lamp, carbon arc	----
2 Gas excitations	vapour lamps, lighting, auroras	----
3. Vibration and rotation	water, ice, iodine, blue flame	----
4 Transition metal compound	Almandine garnet, malachite, turquoise	Crystal field
5 Transition metal impurity	Citrine, ruby, emerald	-do-
6 Colour centre	Amethyst, smoky quartz, maxixe beryl	-do-
7 Charge transfer	Blue sapphire, lapis lazuli	Molecular orbital
8 Organic compound	Amber, coral, graphite	-do-
9 Conductor	Copper, silver, gold, iron	Band
10. Semiconductor	Galena, proustite, pyrite, diamond	-do-
11. Doped semiconductor	blue diamond, yellow diamond	-do-
12 Dispersion	"Fire" in faceted stones	Physical Optics
13 Scattering	Moonstone, "stars" "eyes"	-do-
14 Interference	Iridescent chalcopyrite, iridescent quartz	-do-
15 Diffraction	Opal, labradorite	-do-

Coloured minerals are classified into one of three types *idiochromatic* or *self coloured* - originating from an essential ingredient of the mineral (e.g copper in malachite), *allochromatic* or *other coloured* - originating from an impurity that replaces

essential constituent (e.g. emerald variety of beryl in which chromium replaces some aluminium to produce green colour) and *pseudochromatic* or *false coloured* - originating from physical optical effects (e.g. iridescence in opal and dispersive colours in diamond)

## 6.2 COLOUR OF BERYL

Beryl with a composition of  $\text{Be}_3\text{Al}_2\text{Si}_6\text{O}_{18}$  is colourless. It gains colour due to a variety of reasons (*Table 6.2*). One of the important varieties of beryl is coloured emerald - greened by the impurities of chromium or vanadium, both are frequently present, but there is a lack of agreement as to how emerald should be defined (Sinkankas, 1981; Wood and Nassau, 1968). Neither heat or irradiation affects the chromium or vanadium caused colours (Wood and Nassau, 1968, Sinkankas, 1985), although it is possible to remove traces of yellow, if it is produced by the additional presence of iron (Nassau, 1983 and 1994)

**Table 6.2 : Types of beryl, colour and cause**

Sl No.	Variety	Colour	Cause
1.	Goshenite	uncoloured	no specific cause
2	Heliodor	yellow	UVCT ( $\text{Fe}^{3+} - \text{O}^{2-}$ )
3.	Aquamarine	blue	IVCT ( $\text{Fe}^{2+} \rightarrow \text{Fe}^{3+}$ )
4.	Green beryl	green	UVCT + IVCT
5.	Morganite	pink	$\text{Mn}^{2+}$
6	Bixbite	Red	$\text{Mn}^{2+}$
7	Maxixe	blue	colour centre ( $\text{NO}_3$ )*
8	Maxixe-type	blue	colour centre ( $\text{CO}_3$ )*

\*missing negative charge : hole centre

Apart from being the principal ore of the element beryllium, the allochromatic mineral 'beryl' is known as the source of beautiful coloured gems produced from gorgeous green specimens of emerald, blue coloured aquamarine and other coloured varieties. The colour traditionally associated with aquamarine, or water of the sea is sea green with tinges of blue, but there exists infinite gradations in tone occurring between green and blue shades and some are so pale that they seem colourless until laid on a piece of white paper. A remarkable blue beryl known as '*Maxixe beryl*' occurs in Brazil and is the deepest of all pure blue aquamarine. Colourless beryl are often called '*Goshenite*' found near Goshen, Massachusetts, the name was first applied by the early American Mineralogist, C.U. Shepherd to colourless beryl, but is equally applied to light coloured beryls. '*Helidor*' or literally 'sun glided' is a name originally applied to fine golden beryl from a pegmatite deposit near Rossing, SW Africa by Koloniagesell Schaff für Deutsch-Südwestafrika in 1914. '*Morganite*' is the term applied since the early years of twentieth century to pinkish or lilac variety found in gem mines of S. Carolina and was named by Dr G.F. Kunz in honour of John Dierpont Morgan, a famous gem collector. '*Emerald*' is the term derived from an old Persian which was translated into Greek as "smaaragdus" and is still retained in German. A rare red beryl is also known in nature, and is found as minute crystals in rhyolitic cavities in Utah's Thomas range and Wah Wah mountains (Nassau, 1968). It was named as '*bixbite*' (not to be mistaken for a mineral known as *bixbyite*, composition is  $(\text{Fe, Mn})_2\text{O}_3$ ) by Eppler apparently named after Mynard Bixby - a well known mineral collector of Utah, who found the material (Sinkankas, 1981).

High energy radiations are capable of changing the colour of several minerals and inducing a variety of radiation damage centres which include trapped/missing electrons and or oxidised and reduced cations and anions. Beryls are known to react to high energy radiations and heating in the form of colour change (Pough and Rogers, 1947; Nassau, 1968) Thus deciphering the cause of such colour change by artificial irradiation and heating provide significant insight in unravelling the origin of colour in the host rock (pegmatite) Moreover, changing the colour of an inferior stone to more desirable attractive colour forms an important aspect of *Gem enhancement*, wherein stones of poor quality, lacking attractive colour and clarity (and hence not preferred in the international market) are elevated to desirable colour with the help of artificial irradiation, heating and chemical methods. Beryls found in Orissa are mainly colourless, yellow, light green and pale blue varieties, most of which of inferior quality as far as colour is concerned. An attempt is henceforth made by the author to study the cause of colour and its reaction to irradiation and heating

Before embarking onto the results of each spectroscopic studies, a brief description of various colour changes observed by various workers are discussed.

### **6.2.1 COLOUR CHANGE INDUCED BY HEAT**

Altering the colour of stones by heating is a practice started long time back; however, the history of its beginning are lost in the mists of time. Moreover, altering the colour of stone has always been a trade secret and so not much of it is revealed and published Doetler in 1893, published his *Edelesteinkunde* and included, for the first time, considerable information on colour changes induced in beryls through heat treatment in oxidising and reducing atmospheres He confirmed that the greenish and yellowish beryl

could be changed to blue by heating in an oxidising atmosphere and could be decoloured by prolonged heating.

Jayraman (1940) treated Indian beryls from Nellore, Tamil Nadu and found that upon heating greenish, greenish-blue and greenish yellow beryls to 500 °C for five hours all changed to blue. Subsequently in 1957, Srinivasan heated Nellore, India, blue beryls and found that blue specimens became paler when heated upto 1100 °C. In his opinion blue colour was caused by Fe<sub>2</sub>O<sub>3</sub>, while green was due to FeO. In the year 1952, Frondel conducted heat treatment on variety of beryls and found that emeralds did not change colour upto 1025 °C, the red beryl of Utah also remained unchanged at this temperature, but morganite decolourises at 495 °C. Greenish yellow, olive brown and yellowish green specimens heated in the range of 250 °C- 280 °C, lost their yellow component of green and in turned to blue when heated over 280 - 300 °C. Frondel found that the best blues were obtained from beryls of dark oil-green or olive-green colour, while pale greenish stones provided weak blues. Schmetzer et al.(1975) showed that morganite, coloured by manganese changed to colourless, while the orange variety changed to rose or colourless

## 6.2.2 COLOUR CHANGE INDUCED BY IRRADIATION

Earliest known irradiation experiment on beryl was carried out in 1906, when Miethe subjected Colombian emerald to barium-radium bromide and noted that the colour became paler after several days and finally reached a very pale hue. Pough and Rogers (1945) tested numerous gemstones under X-rays and also found that emerald was unaffected. However, later Pough (1957) observed that, electron bombardment did induce a greenish-grey hue. Schmetzer et al.(1975) found that neither Cr nor V emeralds were affected by X-rays, gamma and electron bombardment, but in some specimens showed a

slight blackening, with development of black specks upon post irradiation heat treatment. In beryls coloured by iron ions, varied changes were observed by many workers. Pough and Rogers (1945) noted that blue aquamarines assumed light to medium green colours, while colourless turned pale brown. Mukherjee (1951) observed pale blue material turned greenish and colourless specimen turned weak brown. A notable discovery was the Maxixe type blue and green beryls by Nassau (1973) from Maxixe mines of Brazil.

Thus a great deal of gem enhancement experiments on beryl has been carried out by various workers. It is well evident that although the colour of minerals of similar specimens may be more or less same through out the world, but the impurities present in them may be varied from place to place which depend on the geological environment at the time of their genesis. Thus in the present thesis, the author describe various colour changes observed on Indian beryls on irradiation and heating with special reference to Orissan beryls (colourless, yellow, light green and pale blue). For a comparative study beryls from Tamil Nadu, Kerala, Siberia and Brazil are also studied. Details of colour changes observed by the author is summarised below.

### 6.2.3 SUMMARY OF COLOUR CHANGES OBSERVED IN THE PRESENT STUDY

1. *Colourless* (Goshenite) - **Maxixe type** (containing colour centre) and **iron** : turns to green to greenish yellow on irradiation → (heating to 300 °C) turns to yellow → (heating to 400 °C) turns to blue → (heating to 500 °C) turns to colourless; unchanged by further heat treatment (*Plates 6.1 a & b; 6.2 a & b*).



Plate 6.1a : Photograph depicting colourless beryl which on irradiation turned to greenish yellow



Plate 6.1b : Photograph depicting irradiated colourless beryl which on heating to 300 °C turned to yellow-orange



Plate 6.2a : Irradiated colourless beryl on heating to 400 °C under controlled conditions turned pale blue. The beryl crystal shown in Plate 6.1 were not heated to 400 °C as it had developed numerous cracks perpendicular to c-axis)



Plate 6.2b : Natural blue beryls from Orissa

2. **Colourless (Goshenite) - Colouring element iron ion:** turns to orange - yellow on irradiation → (heating under controlled conditions to 400 °C) turns to pale blue → (heating to 500 °C) turns colourless; unchanged further by heat treatment (*Plate 6.3*).
3. **Colourless (Goshenite) - Colouring element iron and Manganese:** turns to yellow - orange after irradiation → (heating to 500 °C) turns to colourless, unchanged by subsequent after heat treatment.
4. **Green beryl - Colouring element iron and Chromium:** turns to deep green after irradiation → (heating to 300 °C) turns to light green; turns to blue - green on further heat treatment.
5. **Green beryl - Colouring element iron and Maxixe centre:** turns to deep green after irradiation → (heating to 300 °C) turns to blue green or light green → (heating above 500 °C) turns to colourless.
6. **Yellow beryl - Colouring element iron and Maxixe centre:** turns to greenish yellow on irradiation → (heating to 300 °C) turns to yellow → (heating to 500 °C) turns to colourless, remains colourless on heating above 500 °C.
7. **Blue beryl - Colouring element iron and Maxixe centre:** turns to blue green after irradiation → (heating to 300 °C) turns to blue → (heating above 600 °C) turns colourless; Heating above 600 °C remains colourless.
8. **Blue beryl - Colouring element iron:** Yellow after irradiation → (heating to 400 °C) turns to blue → (heating above 600 °C) turns colourless; Colourless on heating above 600 °C.
9. **Deep blue beryl (T.N) - Colouring element iron:** unchanged after irradiation; Bleaches on heating to above 1000 °C



Plate 6.3 : Irradiated colourless beryl (reveal change of colour from colourless to green to yellowish green and yellow-orange, dark coloured crystals are quartz sample)

Most significant colour change observed by the author were on colourless beryl; which on irradiation with electron beam, some turned to orange - yellow and some to green to greenish yellow (*Plate 6.3*). Although changes to yellow orange has been reported by many previous workers as explained earlier, the change to green to greenish yellow is being observed for the first time (Mathew, et al., 1998). On heating the green colour gets transformed to yellow at 300°C, on further heating to 400°C changes to blue and finally to colourless on heating above 500°C. The author observed that the blue colour formed on heating to 400°C is produced only on heating at controlled conditions, otherwise transforms directly from yellow at 300°C to colourless at higher temperatures.

The above finding of in colourless beryl by the author is useful from commercial point of view, but for a researcher it is the important reason to decipher as to why such colour is produced. Therefore, to understand the cause of colour change in beryls, the author has employed mainly three spectroscopic techniques viz. Electron Spin Resonance (ESR), Optical Absorption Spectroscopy (OAS) and Mössbauer spectroscopy, supplemented by chemical analysis using EPMA.

In the following discussions the results of each spectroscopy is analysed individually with a brief introduction of each spectroscopic techniques.

All the samples were treated with two radiation sources namely,  $^{60}\text{Co}$  gamma rays and electron beam. It was found that gamma ray irradiation could not induce any colour change. Electron beam radiations were carried out using **Cavity Resonator type Linear Accelerator (model ILU6)** housed at Isotope division, BARC, Mumbai, India. The beam current was maintained at 2mA and the samples were kept on water cooled conducting aluminium target to prevent undue heating of the sample.

### 6.3 ELECTRON SPIN RESONANCE

Electron spin resonance (ESR), also called the Electron paramagnetic resonance (EPR) is a spectroscopic technique which considers transitions between sub levels of the atoms, arising due to superposition of an external magnetic field. These transitions correspond to the microwave - radiowave frequency region of the spectrum. The fundamental principle of ESR spectroscopy is that an electron has a spin together with an associated magnetic moment. If the electron is present in a molecule with an  $s$  - ground state, an applied magnetic field will lift the degeneracy ( $\pm 1/2$ ) by causing the magnetic moment to align together either parallel or antiparallel to the applied magnetic field (Figure 6.1). ESR was first discovered by Zavoisky in 1945, but its application to mineralogy commenced only after two decades.

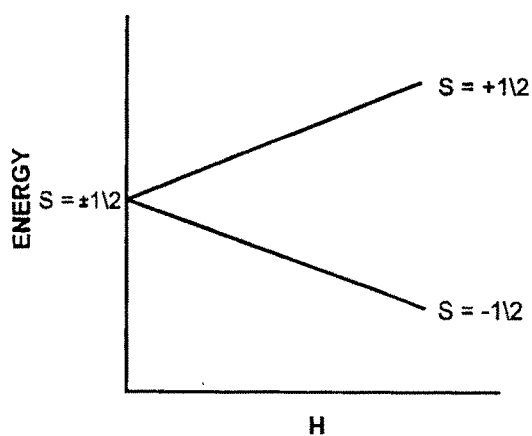


Figure 6.1 : Splitting of a degenerate electronic level ( $\pm 1/2$ ) by a magnetic field.

The conditions necessary for obtaining the resonance is equality of the radio frequency quantum  $h\nu$  ( $h$  is Planck's constant,  $\nu$  is frequency) and the energy difference between spin sublevels, amounting to  $g\beta H$  ( $g$  is a factor of spectroscopic splitting that takes account of the contribution of the orbital and spin moments to the state of the atom;  $\beta$  is Bohr magneton;  $H$  is the intensity of the resonance magnetic field (Calas, 1988; Marfunin, 1979a).

$$h\nu = g\beta H$$

The equation establishes the following :

1. Magnetic field  $H$  brings forth the appearance of spin sublevels and determines the energy difference between them.
2. The radio frequency energy quantum  $h\nu$  causes transition from the lower spin level to the upper one by absorption of energy, and produces an absorption signal.
3. The  $g$  - factor (also called  $g$  - value) defines the change in the position of the absorption line in the spectrum under given  $h\nu$  and  $H$ .

Thus ESR spectrum itself registers  $H_{res}$  values of the magnetic field with which a resonance absorption signal is observed. The absorption line commonly is recorded in the form of an absorption line derivative. ESR spectrum is described mainly by three groups of parameters : a) parameters of initial splitting (the effect of crystal field); fine structure parameter; b)  $g$  - factor (splitting by the applied magnetic field), and c) hyperfine structure parameters (interaction with the magnetic moment of the nucleus).

A typical ESR spectrometer consists of a Klystron or an electron tube, two circular magnets on either side of the sample capillary, oscillograph and recorder. A typical Varian model ESR spectrometer used by the author housed at RSIC, IIT, Mumbai is depicted in *Plate 6.4*.

In mineralogy, ESR studies are concerned mainly with paramagnetic species, which typically are of two kinds: either transition-metal (or rare earths) ions substituting for a diamagnetic host ion or radiation defects (electron-hole centres) formed by natural radiation due to radioactivity or by subsequent artificial irradiation. Further ESR is useful in the determination of the following, a) oxidation state of an ion; b) determination of site occupancy, when trace element incorporation takes place in minerals comprising multiple sites (this cannot be solved by structural refining or EPMA analysis); c) local distortion around the substituting element; d) structural properties, deformation and phase transitions; e) geothermometry and f) ESR dating.

### ***EXPERIMENTAL DETAILS***

Using external morphology and conoscopic interference figure, the samples were cut parallel ( $H||c$ ) and perpendicular ( $H\perp c$ ) to  $c$  axis having dimensions of about 1.5X1.5X10mm placed in a capillary for ESR measurements. ESR measurements were carried out on a Varian E-112, E line century series X-band ESR spectrometer which utilises 100kHz field modulation. *Tetra Cyano Nitro Ethylene* (TCNE,  $g = 2.00277$ ) was used as a standard for  $g$ -factor measurements. Varian variable temperature accessory was used to carry out experiments at different temperatures.

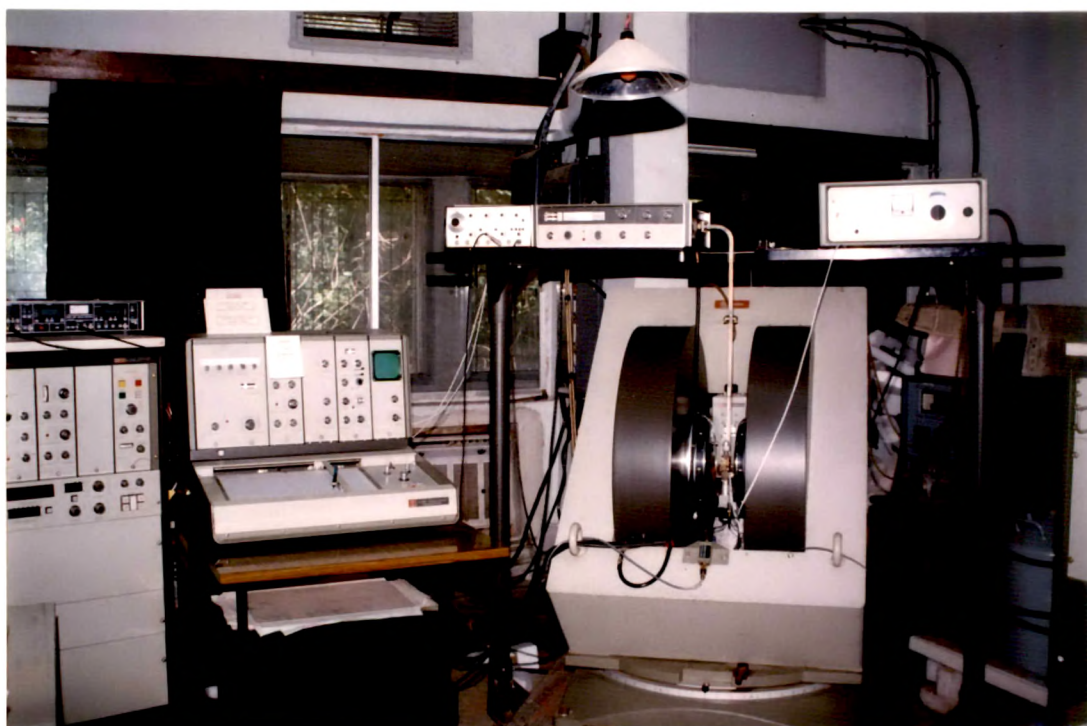


Plate 6.4 : ESR spectrometer at RSIC, IIT, Mumbai

### 6.3.1 ESR STUDIES ON UNIRRADIATED BERYLS

It was long thought that the beryls are colourless due to the absence of colour causing impurities (Sinkankas, 1981, 1985) and the presence impurities such as of iron induce colour. Wood and Nassau (1968) attributed green colour due to presence of  $\text{Fe}^{2+}$  in the channel site, resulting in blue colour and  $\text{Fe}^{3+}$  in the substitutional octahedral Al site resulting in yellow colour. A combination of two would thus result into green.

In the present study, reveals the presence of paramagnetic ion in the ESR spectra of an unirradiated colourless beryl for both the magnetic field directions ( $H||c$ ) and ( $H\perp c$ ) (*Figure 6.2*). Similar spectra were also reported by Davir and Low (1960) and Blak et al. (1982) for coloured beryls. Davir and Low (1960); who were the first to study ESR of beryl proposed that  $\text{Fe}^{3+}$  ion occupy octahedral  $\text{Al}^{3+}$  site and also indicated its probability in tetrahedral site. The spectra (*Figure 6.2a*) of Orissan uncoloured beryl consists of a large asymmetrical single line (labelled 'b') near the free electron resonance region (3200 Gauss or ' $g$ ' = 2.00233), and is attributed to  $\text{Fe}^{3+}$  ion occupying the channel site (' $g$ ' = 1.996 for  $H$  parallel and ' $g$ ' = 1.998 for  $H$  perpendicular to  $c$ -axis) for the following reason.

The above observed ' $g$ ' value for the  $\text{Fe}^{3+}$  ion is close to the free electron ' $g$ ' value of 2.00233. The  $\text{Fe}^{3+}$  in the channel is surrounded by 24 oxygens atoms and the distance between  $\text{Fe}^{3+}$  and an oxygen atom is 3.4 Å in the  $\text{SiO}_6$  plane and 4.1 Å in the plane of  $\text{O}_6$  (Blak et al., 1983). These distances are too large to allow the occurrence of any significant crystal field splitting in the ESR spectra and consequently in the ESR absorption. Therefore,  $\text{Fe}^{3+}$  with a ' $g$ ' value close to 2.0000 behaves almost as a free ion, and thus it probably occupies a site in the channel of beryl lattice (*Figure 3.2*). The broadness of this line is possibly on account of the unresolved super hyperfine splitting lines of  $\text{Fe}^{3+}$  (Calas, 1988)

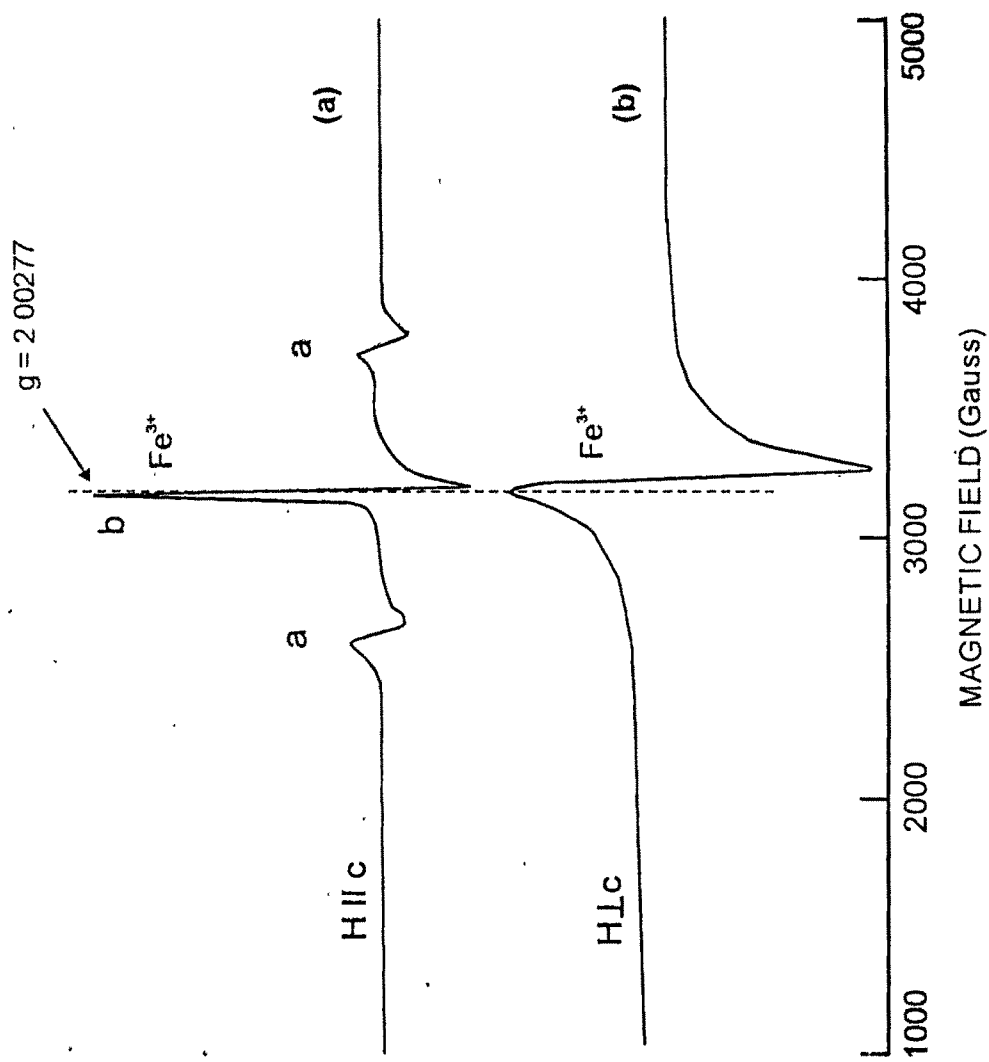


Figure 6.2 : ESR spectra of colourless beryl (before irradiation) along a) HIIc and b) HIc depicting presence of Fe<sup>3+</sup> ion at 3200 Gauss

Additional lines (labelled 'a' in *Figure 6.2*) are observed on either side of the strong line only in the case for H||c. These weak lines are possibly due to the presence of Fe<sup>3+</sup> substituting in the octahedral Al<sup>3+</sup> site as suggested by Davir and Low (1960). The assignment of these two weak lines is still ambiguous (could also be the satellite of the strong Fe<sup>3+</sup> line, Dr. T. K. Gundu Rao, Personal. Comm.). The above observation thus indicates that, colourless beryl do also contain transition impurities, but yet the presence as Fe<sup>3+</sup> ion in channel site does not induce any significant colour.

Similar spectra were also observed for other coloured beryls (the intensities of Fe<sup>3+</sup> are not compared). The presence of Fe<sup>3+</sup> around 3200 Gauss in the channel site is further supported by the angular variation studies (*Figure 6.3a & b*) on single crystal ESR analysis for the 3200 Gauss line in the plane perpendicular to *c* axis and angular variation of the single crystal ESR analysis for the 3200 Gauss line in the *ac* plane. The presence of six fold symmetry (*Figure 6.3a & b*) indicates that this line is due to a paramagnetic centre in the structural channels.

A further supportive evidence corroborating the presence of Fe<sup>3+</sup> line around 3200 Gauss to channel site is observed in one of the light green beryl randomly selected by the author for ESR studies (*Figure 6.4a*). The ESR spectra of this green beryl shows no absorptions peaks around 3200 Gauss region (also no lines attributable to Cr or V), except for a small peak around 1600 gauss and yet the sample is green coloured. *Figure 6.4b*, represents ESR spectra of another green beryl indicating presence of both 1600 and 3200 Gauss peak. Thus the above observation supports the view of Nassau (1994) that the presence or absence of Fe<sup>3+</sup> line around 3200 gauss do not have any effect on colour of beryl crystals, as it is present in the channel site.

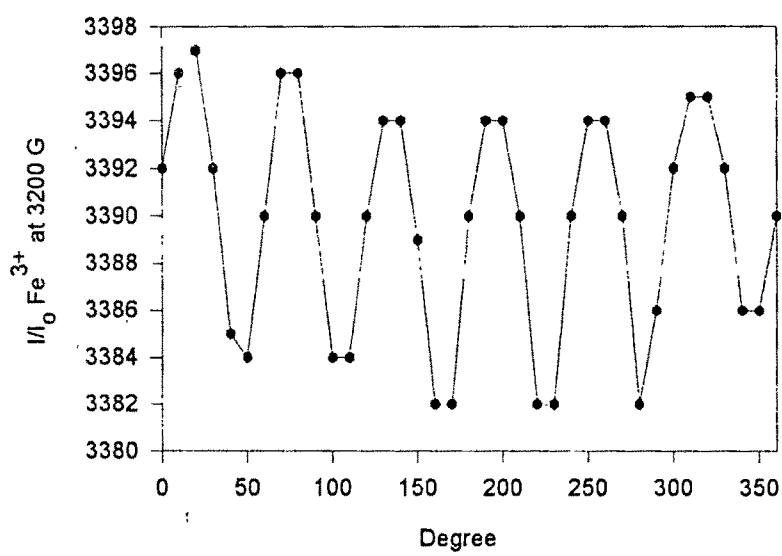
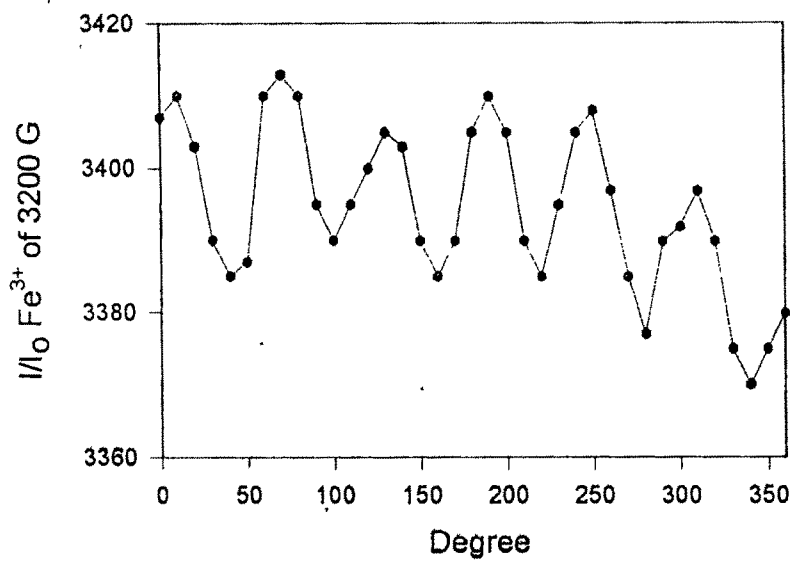


Figure 6.3 : Single crystal ESR angular rotation study along a) H11c and b) H11c of the 3200 Gauss line

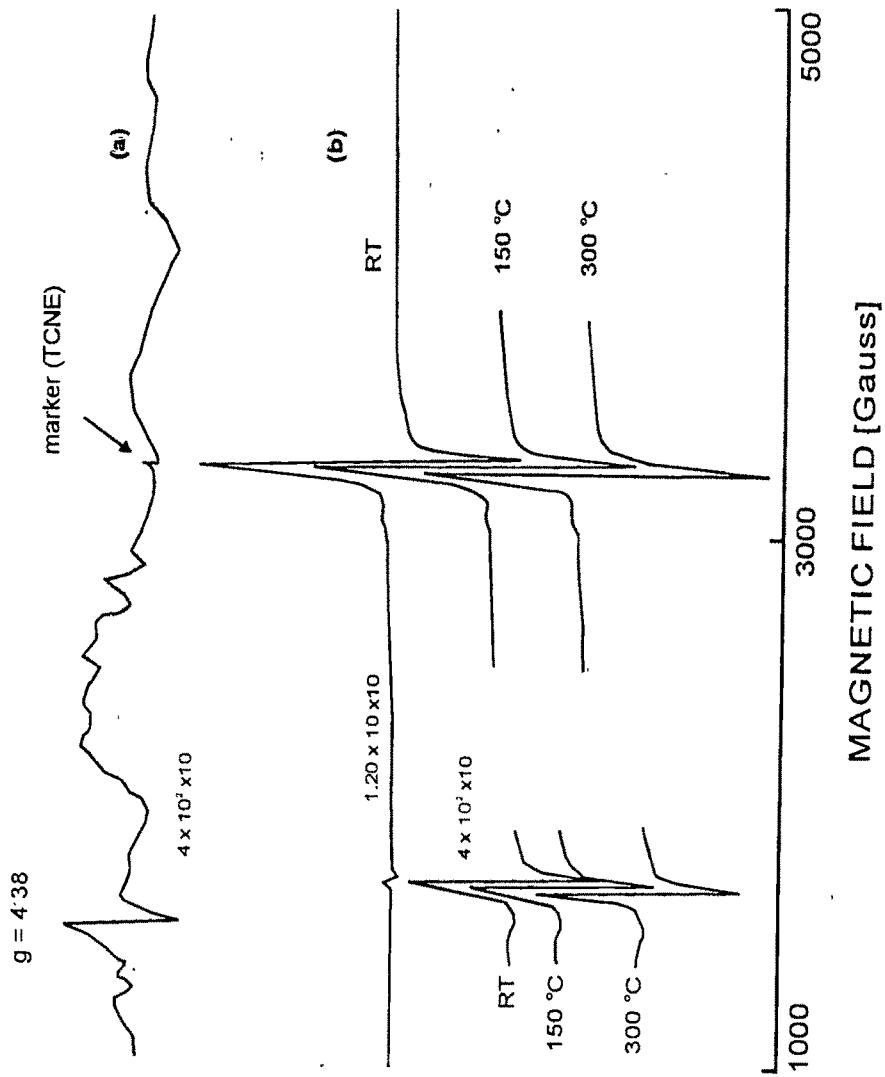


Figure 6.4: a) ESR spectra of light green beryl depicting absence of  $Fe^{3+}$  line at 3200 Gauss and presence of  $Fe^{3+}$  line near 1500 Gauss, b) representing  $Fe^{3+}$  line both at 3200 Gauss and 1500 Gauss in green beryl

The small peak around 1600 gauss (*Figure 6.4a & b*) were also reported by Blak et al (1983) in green beryl from Brazil. They attributed this line to  $\text{Fe}^{3+}$  substituting either at Al, Be or Si site, and remains unaffected on heating. In the present study, the green beryl sample containing both 1600 and 3200 Gauss peaks were heated to 300°C. The peak around 1600 gauss retained its original intensity, which is in accordance with the observations of Blak et al. (1983). For further checking the above observation two deep green beryls were also studied, which also revealed similar behaviour. However, in one of the green beryls (*Figure 6.5*) apart from the  $\text{Fe}^{3+}$  line at 3200 and 1600 Gauss, six lines of equal intensity with equidistant spacing were observed. This line is attributed to the hyperfine splitting of  $\text{Mn}^{2+}$ . The number of hyperfine structure lines determines the spin  $I$  of the nucleus, the number of lines is  $2I+1$ , for  $\text{Mn}^{57}$  with  $I = 5/2$  gives six hyperfine structure line (Marfunin, 1979; Calas, 1988).

The variable temperature ESR study on unirradiated beryl crystals from room temperature (RT) through 150 °C to 300 °C reveal that initially both  $\text{Fe}^{3+}$  peaks (a & b in *Figure 6.6*) increase in intensity upto 150 °C. This is interpreted to be due to partial oxidation of  $\text{Fe}^{2+}$  to  $\text{Fe}^{3+}$ . Subsequently from 150 °C to 300 °C, there is decrease in intensity of  $\text{Fe}^{3+}$  peak indicating partial reduction of  $\text{Fe}^{3+}$  to  $\text{Fe}^{2+}$  (*Figure 6.6*). However, these changes are not accompanied by any colour change. Isotani et al. (1989), showed through kinetic analysis that the above reduction of  $\text{Fe}^{3+}$  to  $\text{Fe}^{2+}$  stops at 200 °C in Brazilian green beryl. However, the authors observation on Indian beryls indicates that the reduction does takes place even beyond 300 °C. However, due to lack of facility to heat insitu beyond 300°C, further heating studies could not be carried out. Heating outside the ESR cavity would result in change in orientation of sample. Even slightest of orientation change in orientation greatly perturbs the intensity and therefore, not correct to be compared with the original intensity.

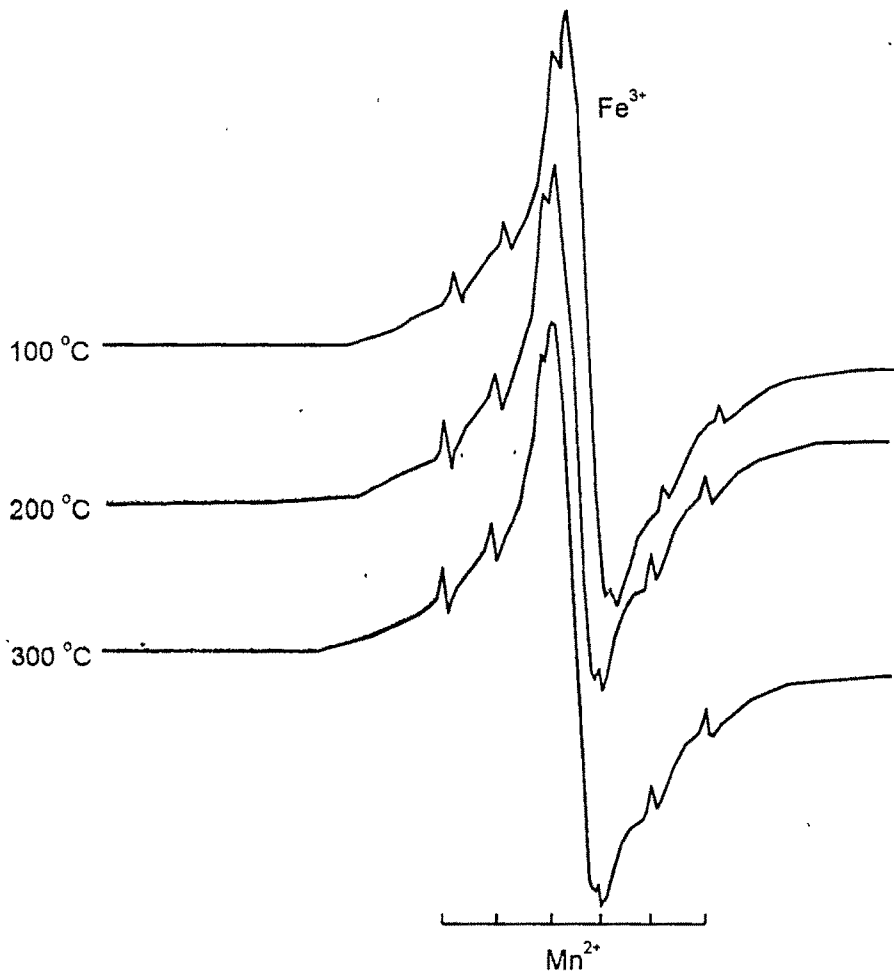


Figure 6.5 : ESR spectra of green beryl showing presence of  $\text{Mn}^{2+}$  hyperfine lines along with  $\text{Fe}^{3+}$

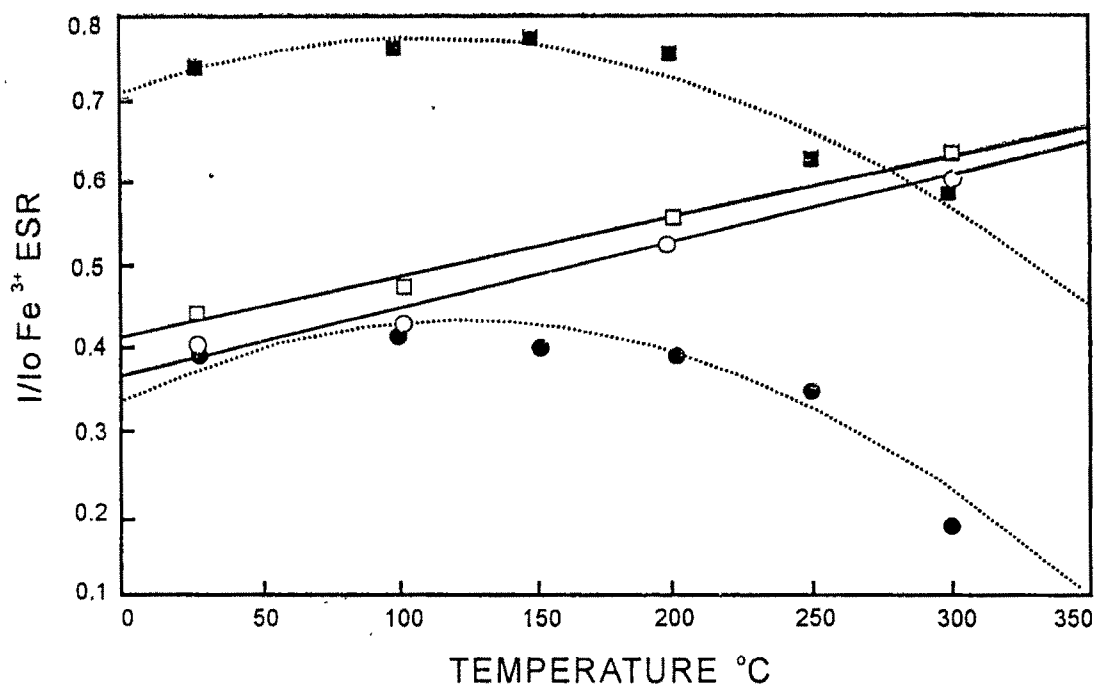
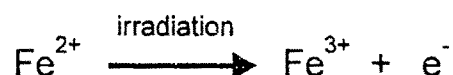


Figure 6.6: Graph depicting behaviour of variable temperature ESR spectral line of  $\text{Fe}^{3+}$  at 3200 G ('b') and small lines ('a') before irradiation (dotted line) and after irradiation (continuous line)

### 6.3.2 ESR STUDIES ON IRRADIATED BERYL

It was observed that in the irradiated beryls, the ESR signal intensities of  $\text{Fe}^{3+}$  ions present at both octahedral and channel sites continuously increase in intensity upto  $300^\circ\text{C}$  (Figure 6.6) Whereas in the unirradiated beryl samples, there is reduction in intensity after  $150^\circ\text{C}$ . The reason for this particular behaviour of  $\text{Fe}^{3+}$  ions in unirradiated and irradiated beryls is not clear.

As mentioned before the uncoloured (goshenite) beryl samples from Orissa turned to green to greenish yellow and some to orange - yellow after irradiation using electron beam, whereas gamma radiation did not produce any colour change. Figures (6.7a & b) show the ESR spectra of irradiated beryl for the magnetic field along the  $c$ -axis and for a random orientation in the plane perpendicular to the  $c$ -axis respectively. In addition to the main  $\text{Fe}^{3+}$  peak at 3200 Gauss, an additional line is observed in the low field region around 1500 Gauss. Such lines reported by Blak *et al.* (1982) in natural green beryl were also observed in the present study in unirradiated green beryl sample (Figure 6.4a & b). They are, however, observed in the present study for the first time in natural beryl crystals after irradiation. The  $g$ -factors in the vicinity of 4.3 in many minerals (e.g. feldspars and mica) have been attributed to high spin  $\text{Fe}^{3+}$  in a low symmetry environment of rhombic distorted site (Castner *et al.*, 1960, Abragam and Bleaney, 1970; Calas, 1988). Therefore it is likely that in the beryl sample under study,  $\text{Fe}^{3+}$  ion is occupying a distorted rhombic site. This indicates that the above  $\text{Fe}^{3+}$  ion was initially in the form of  $\text{Fe}^{2+}$  in the unirradiated sample and on subsequent irradiation,  $\text{Fe}^{2+}$  is oxidised/ionised to  $\text{Fe}^{3+}$ .



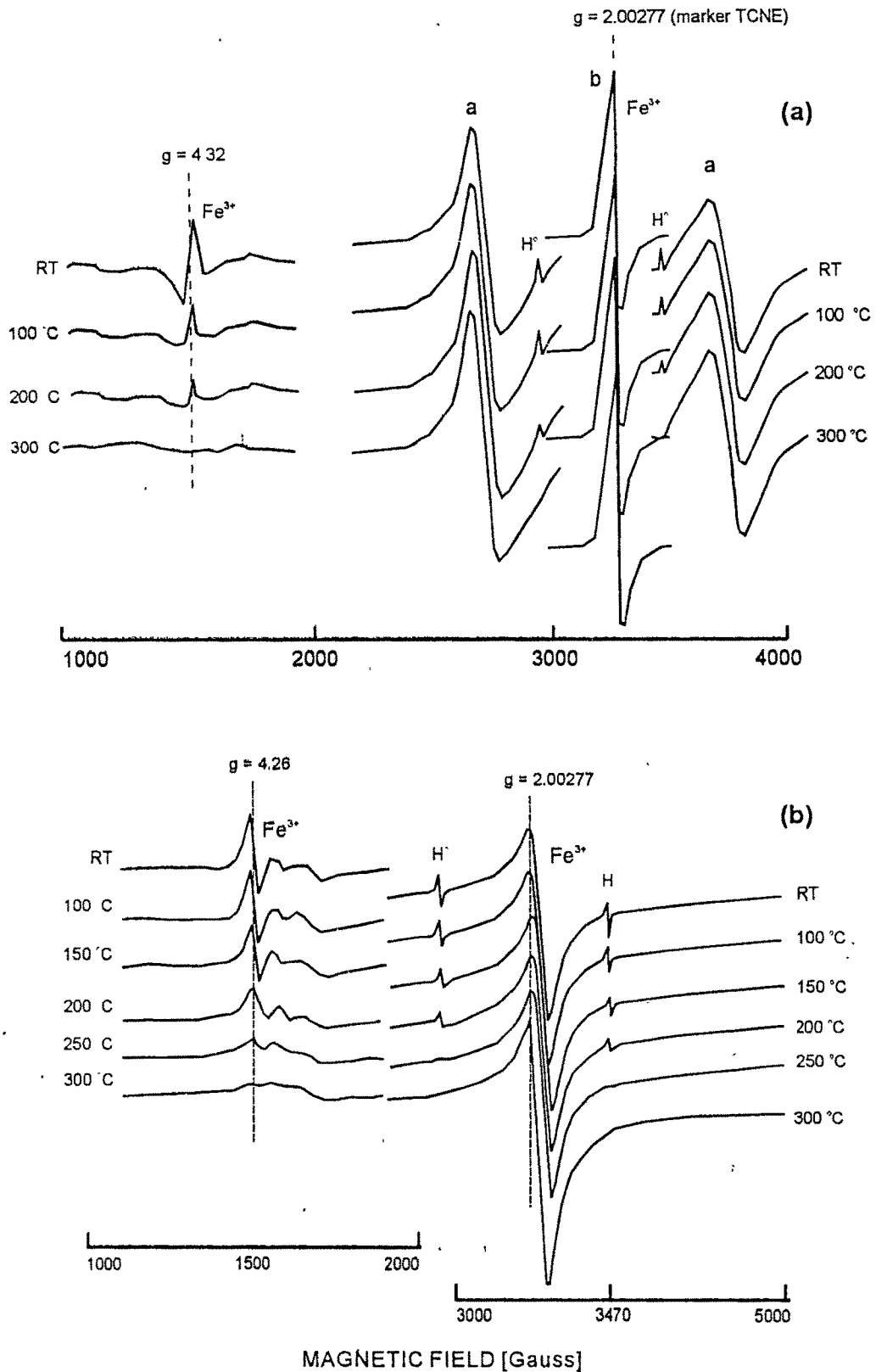


Figure 6.7 : ESR spectra of irradiated colourless beryl along a)  $H \parallel c$  and b)  $H \perp c$ , depicting presence of new line ( $Fe^{3+}$ ) at 1500 Gauss produced only after irradiation, which decays on heating to 300 °C

The ESR lines around the  $g$  - factor of 4.3 (*Figures 6.7a & b*) due to the  $\text{Fe}^{3+}$  ion show a gradual decrease in intensity on heating, which points to a reduction of  $\text{Fe}^{3+}$  to  $\text{Fe}^{2+}$ . The  $\text{Fe}^{3+}$  line at 1500 Gauss disappears around 300 °C and is accompanied by a change in colour of irradiated beryl from greenish yellow to yellow. This observation apparently indicates a possible correlation of this  $\text{Fe}^{3+}$  peak at 1500 Gauss to colouration in irradiated beryl.

A ' $g$ ' value of 4.3 is not expected from an  $\text{Fe}^{3+}$  ion situated at the channel site, since here the ion almost behaves as a free electron ( $g = 2.00233$ ). Its possible substitution at octahedral site is also doubtful, as it is clearly seen in the ESR spectrum that the 4.3 signal of  $\text{Fe}^{3+}$  disappears at 300 °C and yet the sample remain yellow coloured. It is well proved and documented by many authors (e.g. Wood and Nassau, 1968; Samoilovich, 1971, Sinkankas, 1985) that yellow in beryl is due to the presence of  $\text{Fe}^{3+}$  at octahedral site. Further it is known that the bond distances for Be-O and Si-O are 1.657 and 1.608 Å respectively and typical Fe-O bond distances is 1.980 Å (Hazen *et al.*, 1986; Shannon and Prewitt, 1969). It is therefore likely that  $\text{Fe}^{2+}$ , although characterised by large ionic radius, is also substituting in minor quantity at the four-fold co-ordinated beryllium site; while a majority of them prefer the octahedral  $\text{Al}^{3+}$  site and channel site. According to Samoilovich *et al.* (1971) on thermal excitation(heating) of the electron, the capture cross section is greater for the  $[\text{Fe}^{3+}]_{\text{tet}}$  than for the  $[\text{Fe}^{3+}]_{\text{oct}}$  ion. In the present study, step annealing experiments show that  $[\text{Fe}^{3+}]_{\text{tet}}$  is first reduced to  $[\text{Fe}^{2+}]_{\text{tet}}$  below 300°C (*Figures 6.7a & b*). On the other hand,  $[\text{Fe}^{3+}]_{\text{oct}}$  is found reduce to  $[\text{Fe}^{2+}]_{\text{oct}}$  at higher temperatures. These findings are in accordance with the expectations of Samoilovich *et al.* (1971). It was found that the greenish yellow colour as well as ESR signals could be restored after repeated irradiation.

Thus the low intensity line observed around 1500 Gauss in the ESR spectrum (*Figures 6.7a & b*) is assigned to  $\text{Fe}^{3+}$  ion formed by the oxidation of  $\text{Fe}^{2+}$  at the  $\text{Be}^{2+}$  tetrahedral site. As  $\text{Fe}^{2+}$  ion is characterised by a short spin relaxation time, it was not possible to observe the ESR lines attributable to  $\text{Fe}^{2+}$  in the present ESR investigation at room temperature as this would result into broadening of the ESR absorption line. The  $\text{Fe}^{2+}$  lines can be observed only on cooling to 4°K or liquid helium temperature (Vassilikou-Dova, 1987)

The light green beryl on irradiation became deep green. As shown in *Figure 6.8*, the ESR spectra of above green beryl reveals in addition to the main  $\text{Fe}^{3+}$  peak at 3200 Gauss and weak peak around 1640 Gauss ( $g = 3.8$ ), a new line is observed around 1540 Gauss ( $g = 4.26$ ) after irradiation, similar to the observations on colourless beryl described earlier (in colourless beryl the natural line at  $g = 3.8$  is not observed). The peak at  $g = 4.26$  also disappears on heating to 300 °C accompanied by colour change to greenish yellow. Similar spectra were also observed in yellow and blue beryls after irradiation, which turned yellowish and blue green respectively. Some blue beryls changed to yellow on irradiation, however, ESR spectra indicated no notable changes, except for the increase in  $\text{Fe}^{3+}$  peak intensity at 3200 Gauss due to ionisation. On heating the irradiated blue beryl above 400 °C transformed again to pale blue beryl with decrease in intensity of  $\text{Fe}^{3+}$  peak.

The exact intensity difference before and after irradiation of  $\text{Fe}^{3+}$  is not compared in the present study; as heating above 300 °C requires the sample to be taken out of the ESR cavity. This as mentioned earlier, would disturb the orientation of the crystal, resulting into changes in intensity of  $\text{Fe}^{3+}$  peaks. The above reduction of  $\text{Fe}^{3+}$  to  $\text{Fe}^{2+}$  on heating is evident in the optical absorption spectra discussed in the later section on optical spectroscopy

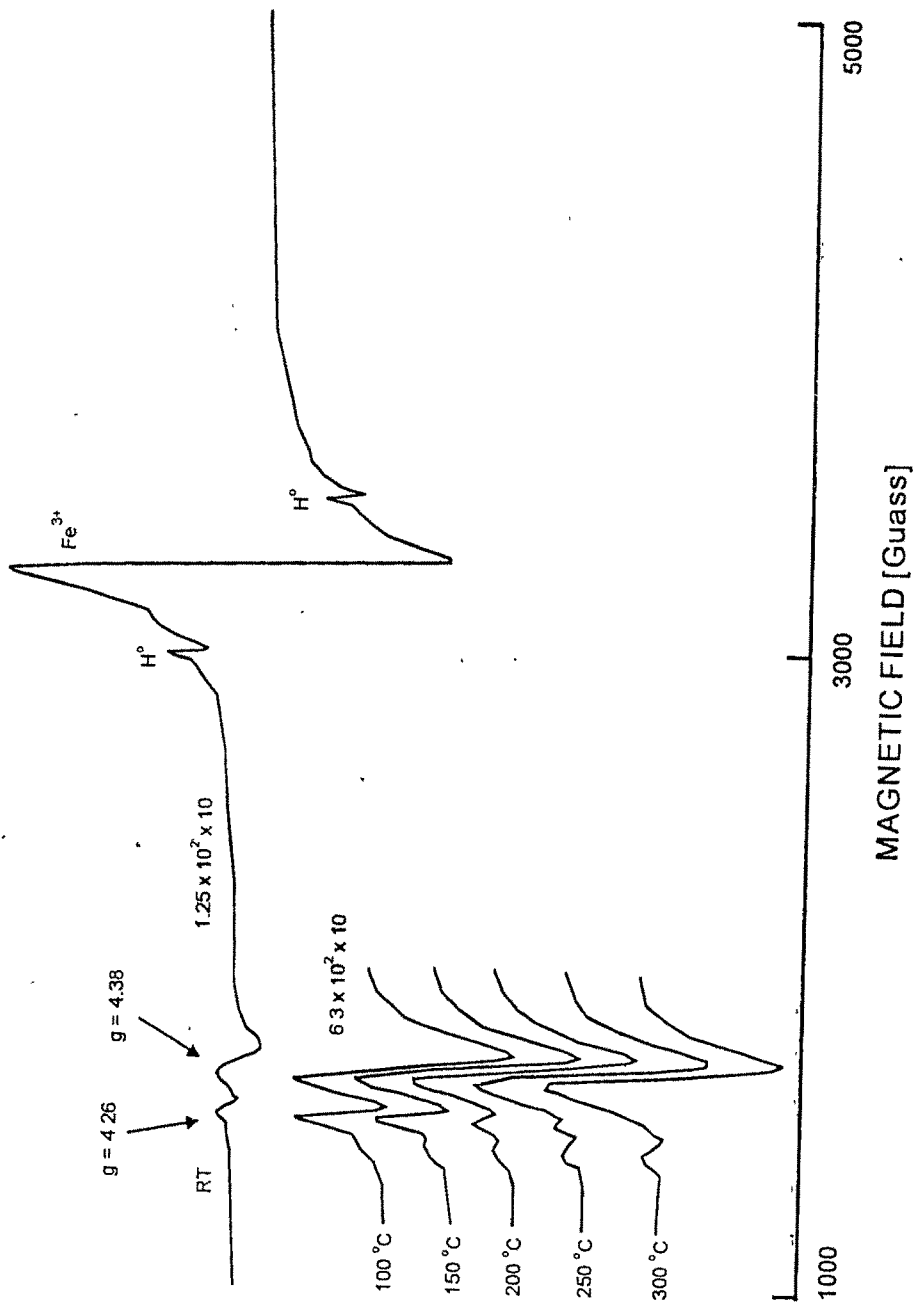
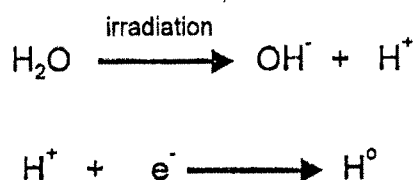


Figure 6.8: ESR spectra of irradiated green beryl indicating presence of new line ( $\text{Fe}^{3+}$ ) at  $g = 4.26$  (1500 G) produced only after irradiation, which decays on heating to 300 °C, the natural line at  $g = 4.38$  is not affected

ESR spectral studies also revealed that, on irradiation with an electron beam, beryl produces atomic hydrogen ( $H^{\circ}$ ) represented by two weak satellites at 2970 and 3470 Gauss (*Figures 6.7, 6.8 & 6.9*). The atomic hydrogen occupies the channel site and appears to be formed by the irradiation induced splitting of the hydroxyl group (Koryagin *et al*, 1966; Bershov, 1970).



The evolving atomic hydrogen can easily diffuse through lattice due to its small size and mobility and become unstable at high temperatures or gets stabilised by traps. On heating the crystal, the trapped hydrogen atoms become free to move and also may be captured by oxygen atoms, which acts as recombination centre (Blak and Mckeever, 1993). In the present study it was observed that  $H^{\circ}$  becomes unstable above 200 °C. Similar weak  $H^{\circ}$  satellites are also observed in samples irradiated by gamma rays, which too disappeared above 200 °C.

One of the beryl after irradiation, in addition to the atomic hydrogen indicated presence of  $\text{CH}_3$  radicals (*Figure 6.9*). The  $\text{CH}_3$  radicals are formed by irradiation induced radiolysis of  $\text{CH}_4$



The C-H bond length in methane is 1.09 Å. This tetrahedral molecule occupies position in the channel (Bershov, 1970) and is found to disappear on heating above 450°C. The presence of  $\text{CH}_3$  in the ESR spectra (*Figure 6.9*) is characterised by four equally

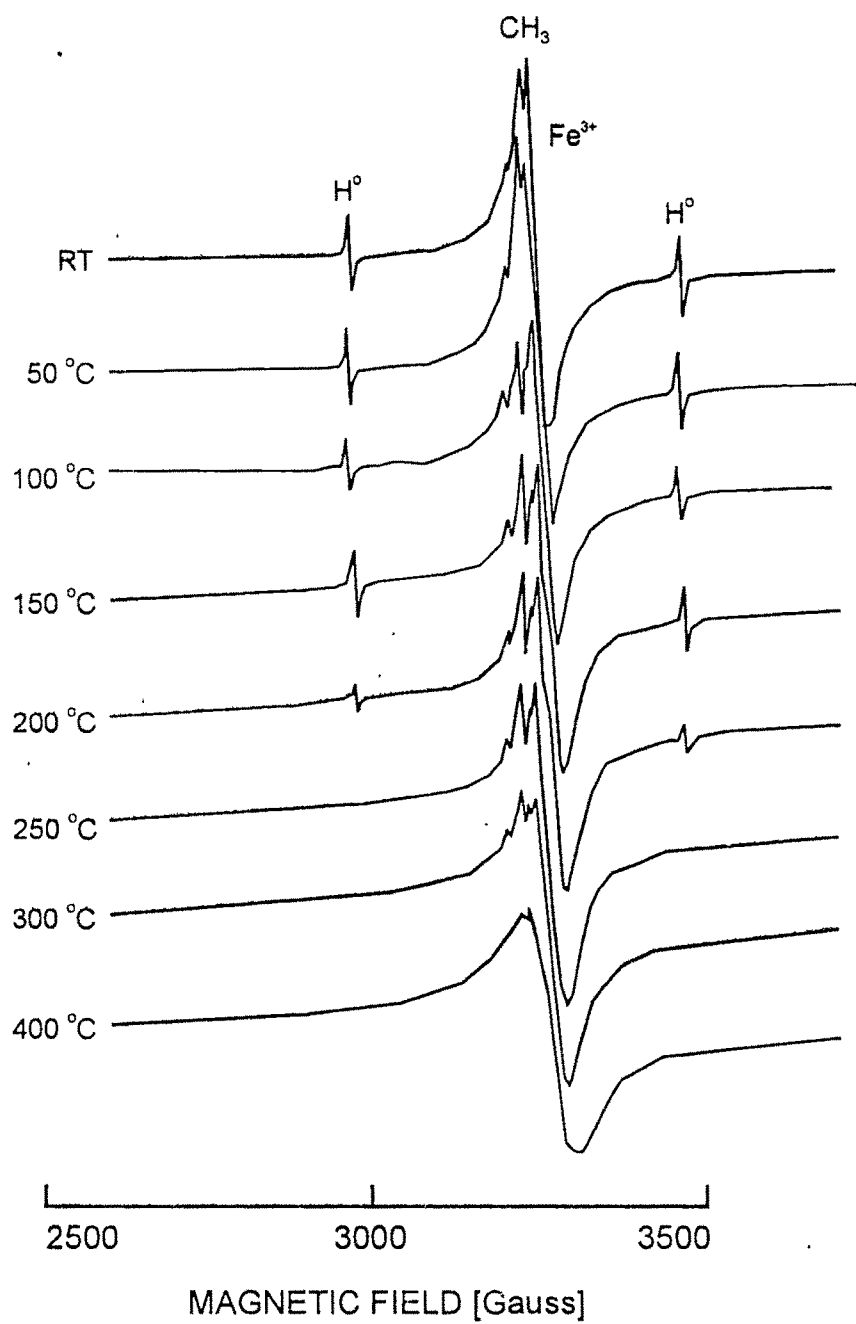


*Figure 6.9* : ESR spectra representing presence of methyl ( $\text{CH}_3$ ) radical produced by irradiation induced scission of  $\text{CH}_4$ , also seen are atomic hydrogen ( $\text{H}^\circ$ ) and  $\text{Fe}^{3+}$  lines.

spaced lines with a separation of 20 Gauss between them (Edgar and Vance, 1977; Marfunin, 1979a; Calas, 1988). *Figure 6.10*, depicts decay curve of both atomic hydrogen and  $\text{CH}_3$  with increasing temperature.

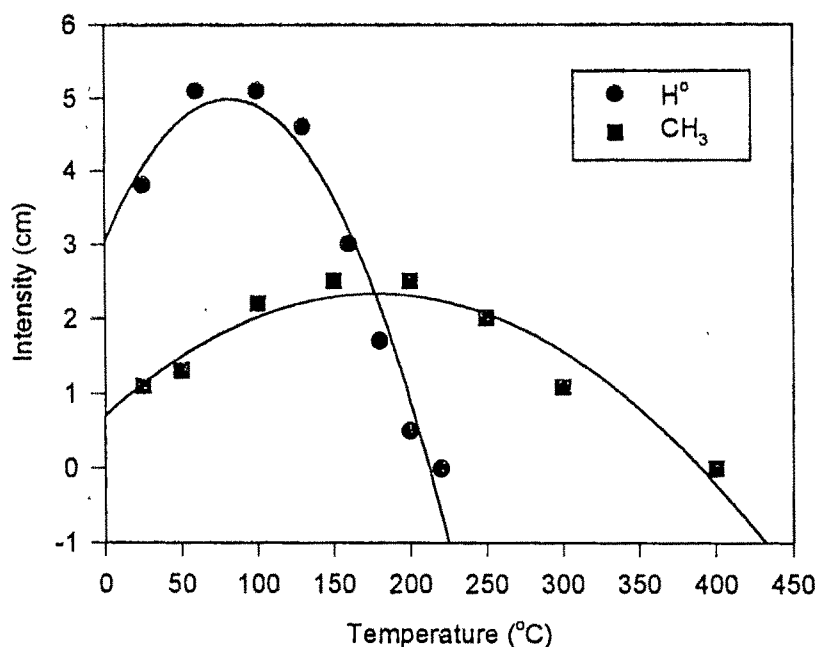
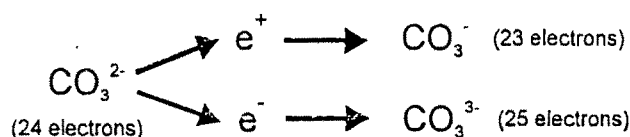


**Figure 6.10 : Thermal decay behaviour of atomic hydrogen ( $\text{H}^\bullet$ ) and methyl radical ( $\text{CH}_3$ ) on heating at higher temperatures**

ESR experiments were also carried out on irradiated beryl crystals (originally colourless) at low temperatures ( $77^\circ\text{K}$ ) to observe the presence of colour centres in the beryl lattice, however, failed to reveal presence of the ESR lines attributable to colour centres due to the strong overlap from the  $\text{Fe}^{3+}$  signal around the free electron resonance region. Nevertheless, its presence was discerned by optical absorption spectroscopy, is discussed in detail by the author in the section on optical absorption spectroscopy.

The optical absorption features revealed (Mathew, et al., 1998) colour centre species similar to *Maxixe type* colour centre delineated by Nassau et al. (1976). The ESR spectral features of above colour centre were, however, observed by Edgar and Vance (1977) and Anderson (1979) in samples with no  $\text{Fe}^{3+}$  impurity. According to these workers the deep blue colour in natural *Maxixe beryl* was due to  $\text{NO}_3$  impurity and in *Maxixe type beryl* (colour produced by artificial irradiation) were due to  $\text{CO}_3^-$  impurity. The ESR spectra of both type of beryls discerned by the above workers are shown in *Figure 6.11*. The  $g$  value for the strong ESR line represented in *Figure 6.11a*, are 2.021 in *Maxixe beryl* and  $2.015 \pm 0.0003$  in *Maxixe type beryl* (*Figure 6.11b*) for the magnetic field perpendicular to  $c$ -axis, and for the field parallel, the  $g$  values are 2.004 and  $2.005 \pm 0.0003$  respectively (Anderson, 1979). Similar  $g$  - values are observed for  $\text{NO}_3$  ( $g = 2.023$  and  $2.003$ ) radical in irradiated  $\text{KNO}_3$  (Livingston and Zeldes, 1964) and for  $\text{CO}_3^-$  ( $g = 2.016$  and  $2.005$ ) in irradiated calcite, which also turned blue (Serway and Marshall, 1967)

As shown in *Figure 6.11a*, the ESR signal has split into three lines. This is characteristic of a nucleus with spin = 1 like in  $^{14}\text{N}$ , while nuclei having spin = 0 (e.g.  $^{16}\text{O}$  and  $^{12}\text{C}$ ), do not split the ESR line (*Figure 6.11b*). These centres are created when  $\text{NO}_3^-$  and  $\text{CO}_3^{2-}$  impurity ions loose one electron or when hydrogen atom is removed from  $\text{HNO}_3$  and  $\text{HCO}_3$  (Anderson, 1979).



The 23 electron,  $\text{CO}_3^-$  radical is isoelectronic with  $\text{NO}_3$  and forms due to the hole trapping (the loss of an electron) by  $\text{CO}_3^{2-}$  radical. By trapping a hole (positive charge) or

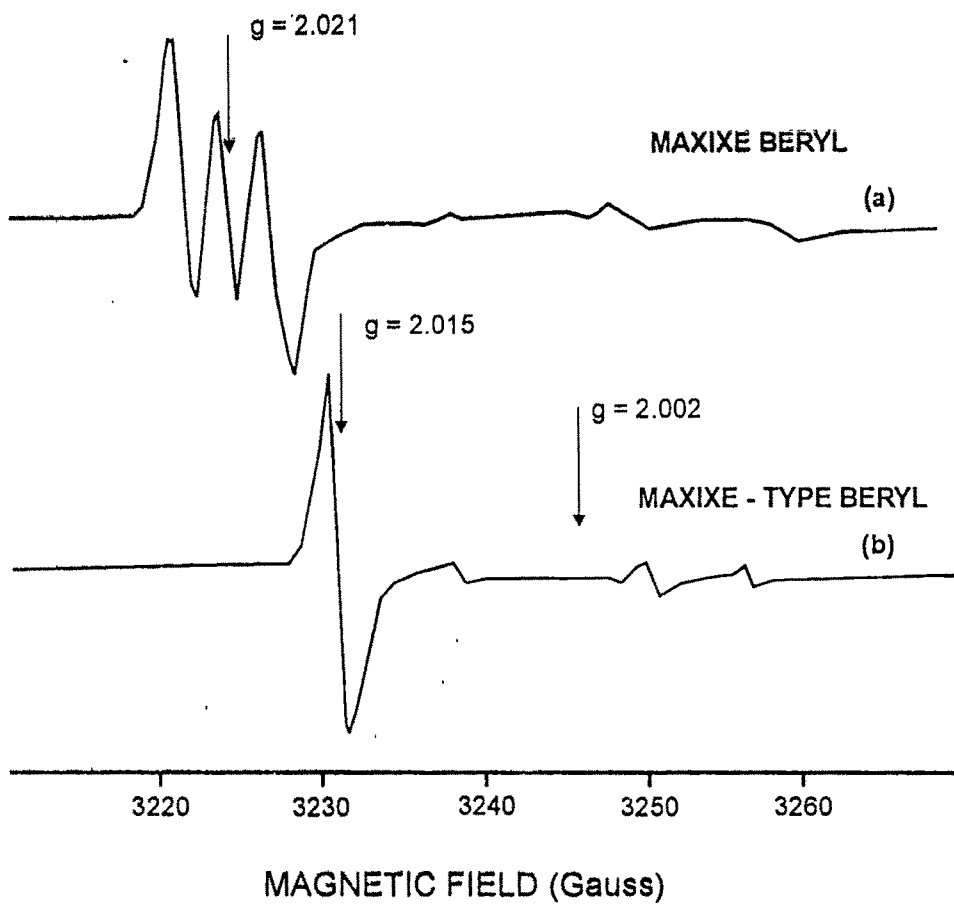


Figure 6.11 : ESR spectra features of, a)  $\text{NO}_3$  radical in Maxixe beryl and b)  $\text{CO}_3$  in Maxixe type beryl (after Anderson, 1979)

an electron the radical  $\text{CO}_3^{2-}$  becomes a free radical. Unlike simple ions, in radicals the electron or hole is captured not by one oxygen or carbon ion, but by the radical as a whole (Marfunin, 1979a). Thus in the  $\text{CO}_3^{2-}$  radical a hole is trapped not on one oxygen ion, but is distributed among all the three oxygens. This kind of an electron distribution leads to an axial symmetry of  $\text{CO}_3^{\cdot}$  (Edgar and Vance (1977)).

Thus the above study by the author based on ESR spectroscopic studies deduce the necessity of  $\text{CO}_3^{2-}$  or  $\text{NO}_3^-$  impurities (*precursors*) in beryl order to produce irradiation induced blue colouration. In order to retain for the colour, the lost electrons have to be strongly trapped. Otherwise would return to the original ion, as they do under the influence of heat or light, causing the colour to bleach. The extent to which a stone can be coloured depends on the concentration of the necessary impurities.

#### 6.4 OPTICAL ABSORPTION SPECTROSCOPY (OAS)

*Optical absorption spectroscopy* (OAS) at times is also referred as *Electron absorption spectroscopy* (EAS) is a spectroscopic technique; in which the wavelength of monochromatic light passing through a crystal corresponds to the difference in energy levels of an ion in the crystal. Absorption of light energy is manifested in the form of absorption band in the optical spectrum of the crystal. Transition from the ground state to the excited state corresponds to the transfer of an electron to one of the excited state configurations or excited state transcribed by ion terms in a crystal field, e.g. in the 'd' orbital, the electron is transferred from 't<sub>2g</sub>' level (d<sub>xy</sub>, d<sub>xz</sub>, d<sub>yz</sub>) to the 'e<sub>g</sub>' level (d<sub>x<sup>2</sup>-y<sup>2</sup></sub>, d<sub>z<sup>2</sup></sub>) separated by the crystal field (Burns, 1993). Absorption bands corresponds to energies of excited levels of ions in the crystal; and optical absorption spectra are basic experimental data for ion level energies in the crystals. Levels of the ions with incomplete

'd' and 'p' shells are only split by the crystal field and the strength of the crystal field for these O ions have such a value that the energy separation between the split levels corresponds to energies of ultraviolet (UV), visible, near infrared (NIR) regions of the spectrum.

Mineral spectra provide information on the electronic energy levels of transition metal ions in polyhedral co-ordination having a variety of symmetries, distortions, bond types and number of nearest neighbour ligands. High thermal stability of most silicates and other minerals make it possible to measure optical spectra of these transition metal bearing phases at elevated temperatures and pressures. These features make mineral spectra interesting for earth scientists to interpret geochemical and geophysical properties of minerals. Optical spectroscopy is thus primarily concerned with transitions of electrons between outermost energy levels

Basically three types of process (theories) are involved in the formation of optical absorption spectra. Each of them can act independently or collectively (Marfunin, 1979; Rossman, 1988, Burns, 1993). These theories are, a) *crystal field theory* (crystal field spectra), b) *molecular orbital theory* (charge transfer spectra) and c) *band gap theory* (absorption edge).

- a) This type of electronic transition involves electrons in the d-or-f orbitals of the ions of the first row transition elements such as  $\text{Cr}^{3+}$ ,  $\text{Mn}^{2+}$ ,  $\text{Mn}^{3+}$ ,  $\text{Fe}^{2+}$  and  $\text{Fe}^{3+}$ . These transition involve rearrangement of valence electrons and give rise to absorption in the visible and near IR region. Such spectra produced are often called *Crystal field spectra*. These electronic transition are major cause of colour in many minerals.
- b) Transition in which electron from one orbital on one atom is promoted to a higher energy orbital on adjacent atom. There are two ways in which this can occur:

- i) electron transfer from anion to cation e.g. transfer from a filled oxygen  $p$  orbital to a partially occupied  $\text{Fe}^{3+}$   $d$  orbital. These transitions occur in the ultra-violet region and produce very intense absorption (upto  $10^3$  to  $10^4$  times) higher than those of crystal field transition. Since such transition are centred around UV region are known as *Ultraviolet charge transfer (UVCT)*. In ions having higher oxidation states such as  $\text{Fe}^{3+}$  or  $\text{Cr}^{6+}$ , the tail of absorption band extends into the visible part of the spectrum, causing absorption strongest in the violet region and extending towards red.
- (i) electron transfer from one cation to a higher energy orbital in adjacent cation. The cations must have different oxidation states and transfer generally occurs between cations in adjacent edge or faces sharing co-ordination polyhedra, having metal - metal interatomic distances small, e.g. black of *magnetite* are due to IVCT between  $\text{Fe}^{2+} \rightarrow \text{Fe}^{3+} / \text{Fe}^{3+} \rightarrow \text{Fe}^{2+}$  and *deep blue sapphire* are due to  $\text{Fe}^{2+} \rightarrow \text{Ti}^{4+} / \text{Fe}^{3+} \rightarrow \text{Ti}^{3+}$ . Such charge transfer mechanism are referred to as *Intervalence charge transfer (IVCT)*. This absorption occurs in the visible region of the spectrum .
- c) Of less importance are absorption resulting from electronic transitions in gap between the valence band and the conduction band (*band gap theory*). Any photon with energy greater than this gap will be absorbed. Blue and yellow colour in diamond is also explained by this theory (Nassau, 1994). Such absorptions are usually seen in sulphides. Band gap of silicate minerals is typically located far in the ultraviolet region.

*Overtone vibrations :*

The most commonly encountered bands in the near infrared are overtone of OH and H<sub>2</sub>O groups. These vibrational overtones are rapidly recognised because they have smaller widths than electronic transitions which can occur in the same spectral region.

The principal features of a typical absorption spectrum in the UV to IR spectral range are shown in *Figure 6.12*.

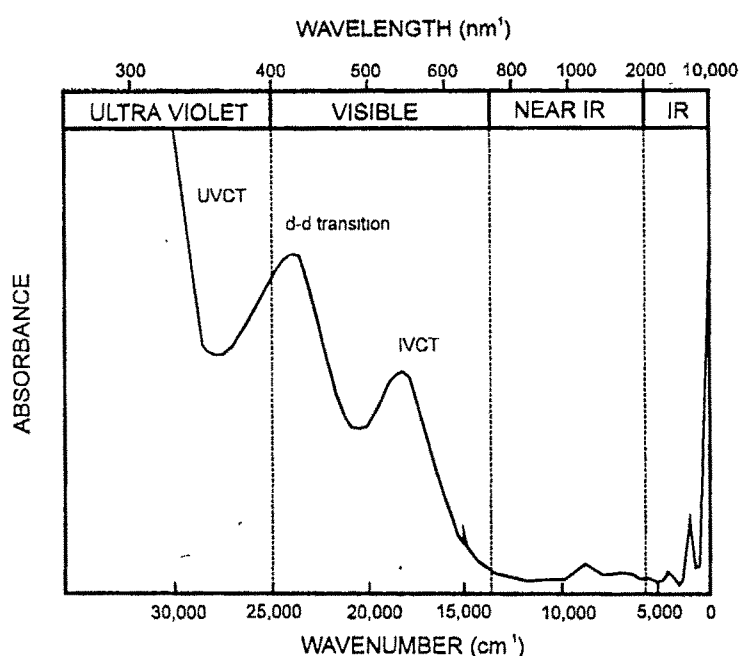


**Figure 6.12 :** Principal features of a typical absorption spectrum in the range from ultraviolet through to the near infra-red.

Certain additional processes are important in the case of few minerals. These are various absorptions associated with *electron-hole centres* and *molecular ions* produced by ionisation radiation. Energy units used in the OAS are often quoted in terms of *wavelength* as well as *wavenumber*.

Thus optical absorption spectroscopy is an effective method to investigate the atomic and electronic structure of minerals.

## **EXPERIMENTAL DETAILS**

Slices were cut and polish with optic axis parallel to polish surface, so that the ordinary ray ( $\omega$ ) and extra ordinary ( $\epsilon$ ) ray spectra could be obtained from single section by the use of polarised radiation. Spectra were recorded in the ultraviolet-visible-near infrared (300 - 2000 nm) on a **Schimadzu UV 3101PC scanning spectrometer**. Polarised sheets HN22 were used to obtain polarised spectra. Heat treatments in air upto 1000°C were carried out using an electric furnace, with samples kept in a nickel crucible.

### **6.4.1 OAS STUDIES ON BERYL**

Colour in beryls (emerald, aquamarine, heliodor, morganite) is a result of absorption in the 400 - 700 nm range. The chief causative agents being chromophoric transition metal ions (*Table 6.2*). In the region beyond 3000 nm, there are absorption due to vibration of crystal lattice. Absorptions in the region from 1000 - 5000 nm are absorptions originating from impurity molecules trapped in the structural channels. *Figure 6.13*, depicts a composite spectrum illustrating various region. Any absorptions beyond the visible spectral range has no effect on colour.

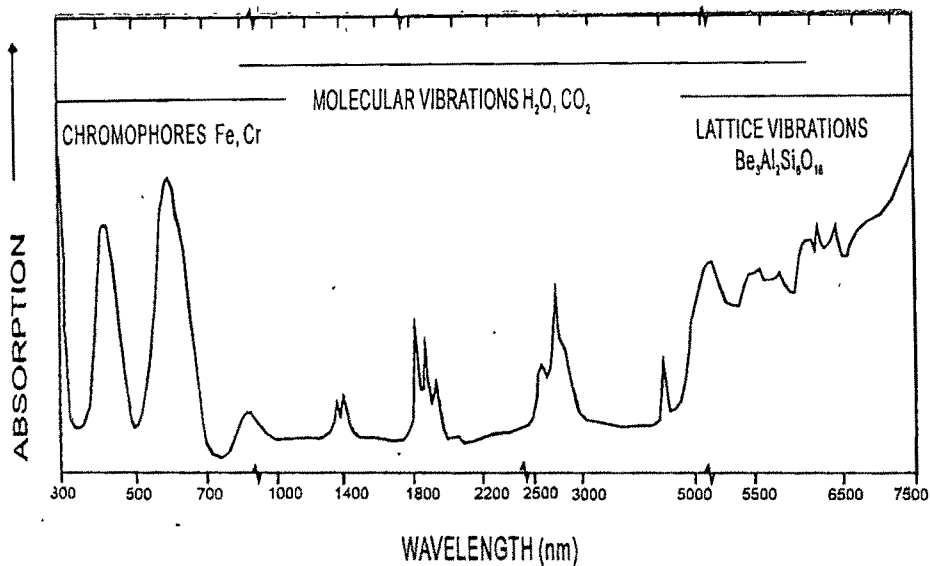


**Figure 6.13 :** Composite spectrum of beryl showing; the region of lattice vibration (4500 - 7500 nm), molecular vibrations ( $\text{H}_2\text{O}$  and  $\text{CO}_2$  (4000 - 5000 nm) and chromophoric absorptions (400 to 700) along ordinary ray (after Wood and Nassau, 1968)

#### 6.4.2 COLOURLESS BERYL (GOSHENITE)

Wood and Nassau, (1968) recognised three absorption bands in the near infrared (NIR) region and attributed them to  $\text{Fe}^{2+}$ . A band near 810 nm in the spectrum of *o* - ray ( $\perp c$ ) was assigned to  $\text{Fe}^{2+}$  in the  $\text{Al}^{3+}$  site. On the other hand, a set of bands near 810 nm and 1000 nm for *e* - ray ( $\parallel c$ ) was attributed to  $\text{Fe}^{2+}$  in the channel site and the band centred at 620 nm ( $\parallel c$ ) was attributed to  $\text{Fe}^{2+}$  in a different site. Samoilovich *et al.* (1971) and Parkin *et al.* (1977) agreed to the assignments of Wood and Nassau, (1968). However, according to Price *et al.* (1976) bands at 810 and 1000 nm ( $\parallel c$ ) arose from  $\text{Fe}^{2+}$  in the  $\text{Al}^{3+}$  site and the 810 nm band ( $\perp c$ ) possibly indicated  $\text{Fe}^{2+}$  at tetrahedral site Goldman *et al.* (1978) attributed 820 nm and 970 nm peaks in the spectrum ( $\parallel c$ ) to  $\text{Fe}^{2+}$  in the  $\text{Al}^{3+}$  site and assigned 820 nm ( $\perp c$ ) and 2100 nm ( $\parallel c$ ) peaks to  $\text{Fe}^{2+}$  in a channel site. They ascribed a broad absorption feature seen from 1700 nm to 2500 nm also to iron in a channel site.

Thus there is no universally agreed point of view regarding the interpretation of optical absorption spectra of beryl Panjkar (1995) also carried out extensive OAS studies on Orissan beryls and indicated possible presence of  $\text{Fe}^{2+}$  band at octahedral as well as tetrahedral site.

As shown in *Figure 6.14*, the optical spectra of colourless beryl reveal no absorption in the region 400 - 700 nm, making the crystal colourless, even though the 820 nm band is very strong. This is because there is essentially no absorption in the region to which the eye is sensitive (420 - 680 nm). Optical spectra of colourless beryl indicates existence of two distinct types of  $\text{Fe}^{2+}$

In the present study, strong absorption due to the crystal field transition of  $\text{Fe}^{2+}$  at 820 nm polarised along ordinary ray (o-ray or  $\perp c$ ) is assigned to  $\text{Fe}^{2+}$  in the channel site (*Figure 6.14*). Since the octahedral Al site is distorted, the  $\text{Fe}^{2+}$  absorption band is expected to be in pairs rather than a single band due either to distortion of the polyhedron or to the dynamic Jahn -Teller effect (Goldman *et al.* 1978, Burns, 1970, 1993, Marfunin 1979; Berry and Vaughman, 1985). This absorption pair feature is seen at 820 and 920 nm polarised along the extraordinary ray (e-ray or  $\parallel c$ ) (*Figure 6.14*). It is attributed to the spin allowed crystal field transition of  $\text{Fe}^{2+}$  ( ${}^5\text{T}_2 \rightarrow {}^5\text{E}, {}^5\text{D}$ ), assigned to arise from  $\text{Fe}^{2+}$  in the octahedral site. This is further supported by the barycentre energy of  $12,150 \text{ cm}^{-1}$ , with *Faye* plot (Faye, 1972) on crystal field parameter versus Al - O bond distance (*Figure 6.15*). It indicates that the  $\text{Fe}^{2+}$  is situated in a site of 1.94 Å average metal oxygen distance. This agrees favourably with the 1.90 Å distance determined for octahedral Al site in beryl by Gibbs *et al.* (1968).

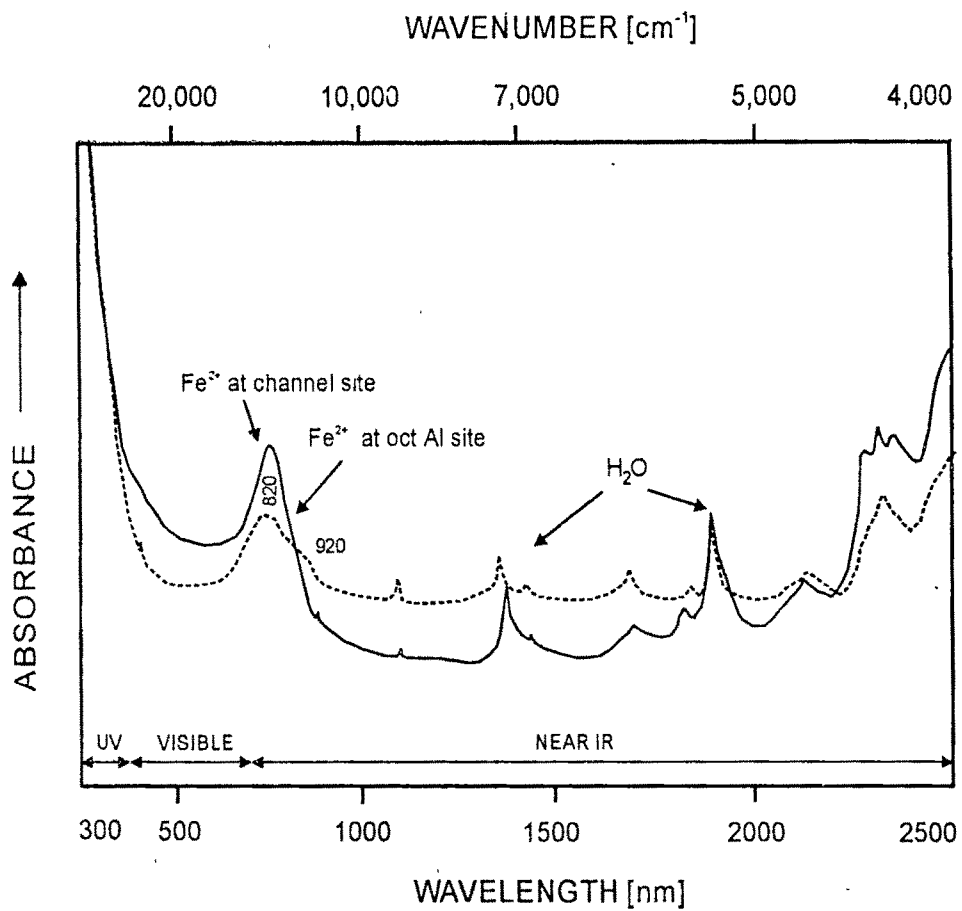
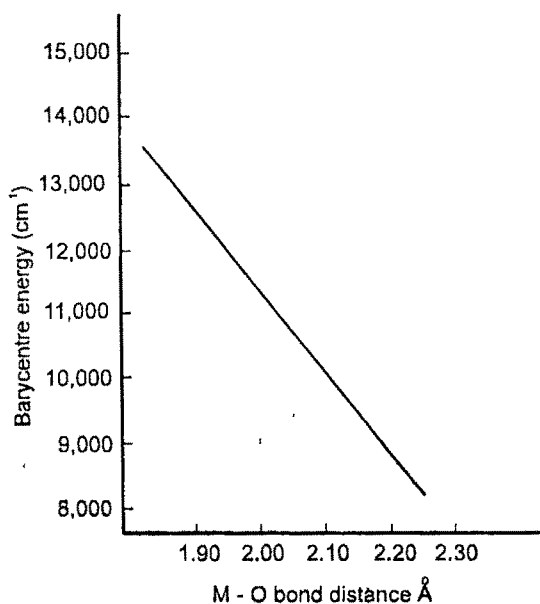


Figure 6.14 : Polarised optical absorption spectra of colourless beryl along o - ray (continuous line) and e - ray (dashed line)



**Figure 6.15 :** Faye (1972) figure illustrating relationship between barycentre energy and bond distance

### 6.4.3 IRRADIATED (GOSHENITE) BERYL

Optical absorption studies of irradiated coloured beryl were carried out at various temperatures. The absorption spectra of irradiated greenish yellow beryl at room temperature (RT) are shown in *Figures 6.16* and *6.17*. It is observed that the ultraviolet charge transfer (UVCT) seen below 390 nm extends into the visible region. This UVCT is due to electron transfer from anion to cation, i.e. transfer of electron from  $O^{2-}$  ligands to central ( $Fe^{3+}$ ) metal ion (Rossman, 1988). These transitions occur in the ultraviolet region and produce more intense absorptions than the crystal field transition (Marfunin, 1979b; Burns 1993) 2 to 3 orders of magnitude higher than the ordinary crystal field transition. The tail of absorption band extends into the visible region due to an increase in concentration of  $Fe^{3+}$  on account of ionisation of  $Fe^{2+}$ . This results in the strongest absorption in UV to violet and extending further towards visible region.

The visible region of the optical spectrum in the irradiated greenish yellow beryl is characterised by a sharp absorptions at 644 and 688 nm, which is observed to be polarised

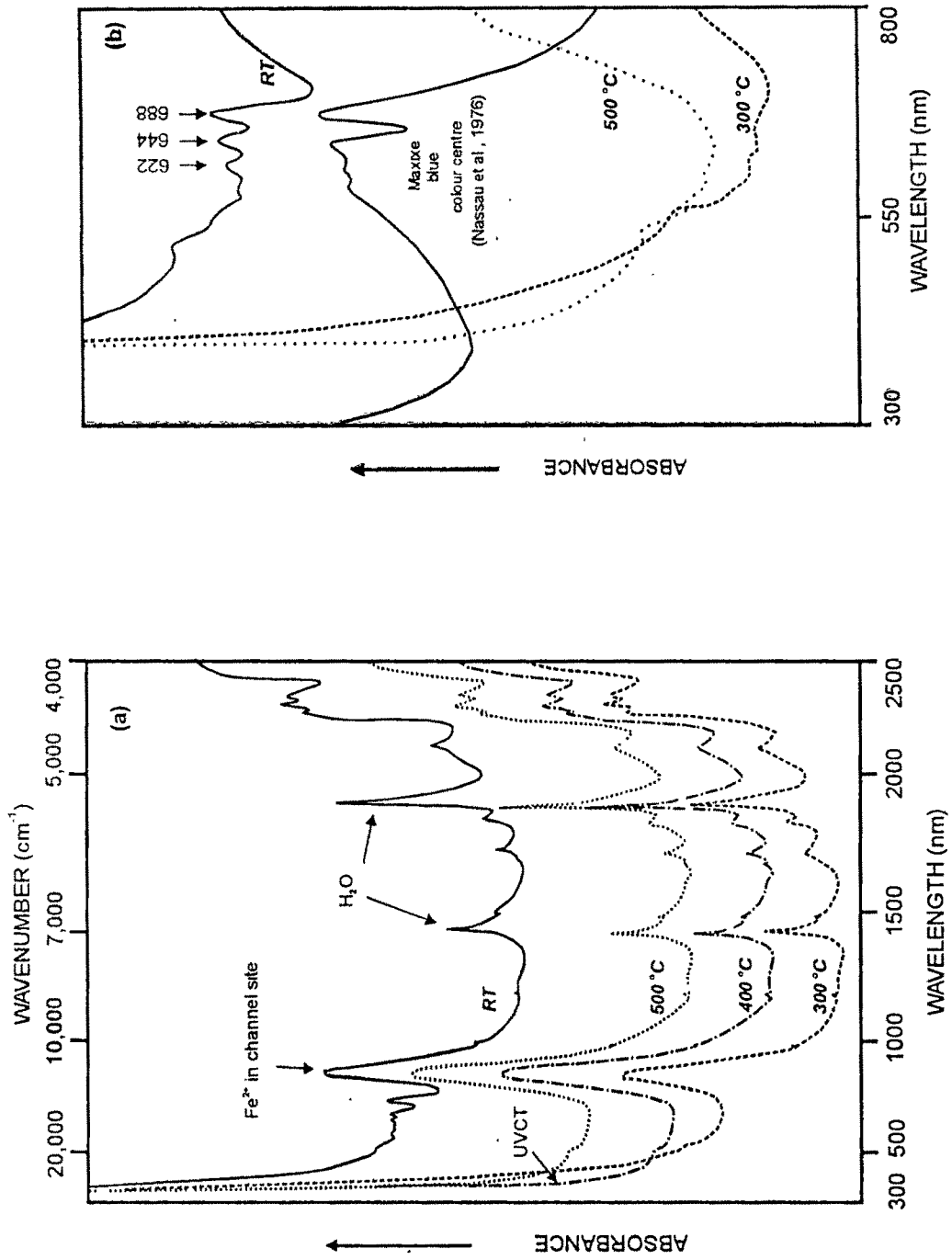


Figure 6.16 : Optical Absorption spectra of irradiated colourless beryl. a) OA spectra along *e*-ray in the UV-VIS range b) OA spectra along *o*-ray in the UV-VIS range depicting presence of Maxixe type colour centre.

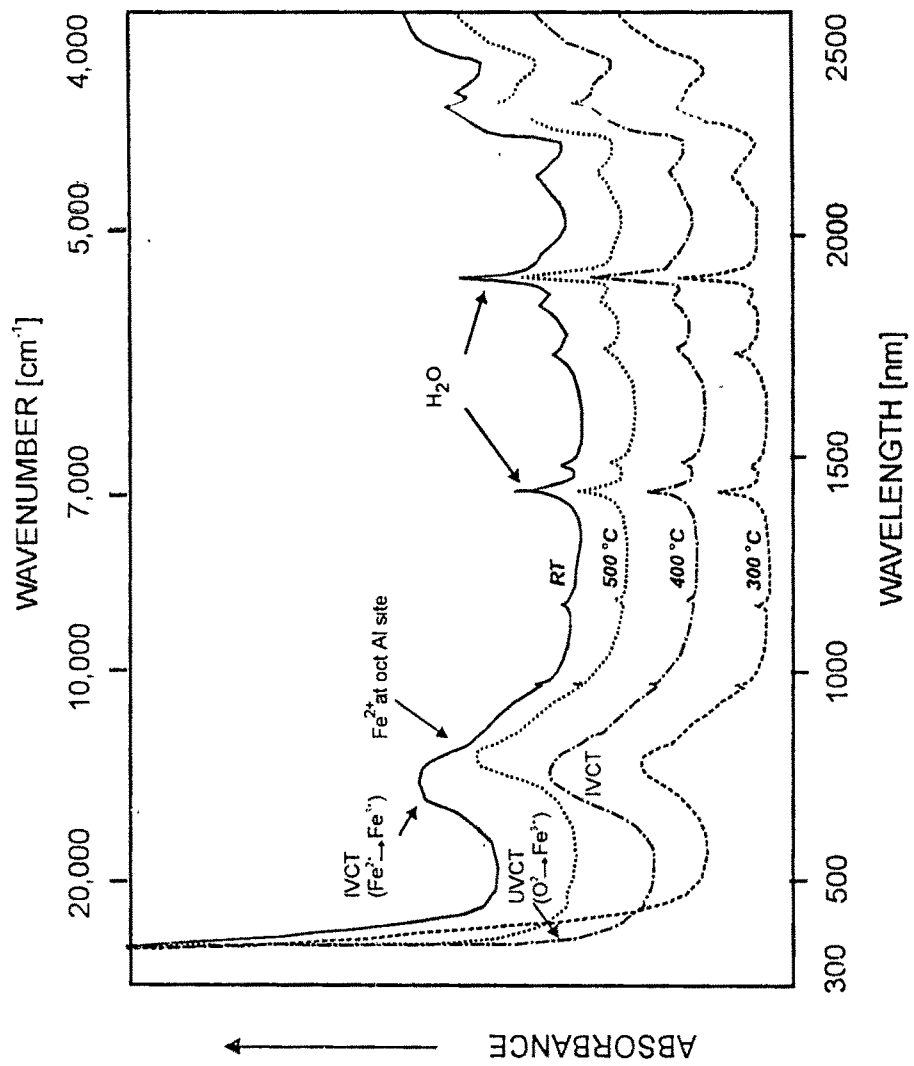


Figure 6.17 : Optical Absorption Spectra of irradiated colourless beryl along e - ray depicting presence of Fe<sup>2+</sup> at octahedral Al site and IVCT band.

only along the ordinary ray (*Figure 6.16b*). Such sharp absorption feature is not seen in the beryl irradiated to yellow-orange. The sharp absorption feature observed above is similar to the optical spectrum of Maxixe type beryl observed by Nassau *et al.* (1976). They attributed this absorbance to colour centre formation and concluded that this was the cause of blue colour in Maxixe type blue beryls from Brazil. Later workers (Edgar and Vance, 1977, Anderson, 1979) with the help of ESR studies, inferred this centre to be  $\text{CO}_3^{\cdot-}$  radical in Maxixe type beryl and  $\text{NO}_3$  in Maxixe beryl. These radicals are derived from  $\text{CO}_3^{2-}$  and  $\text{NO}_3^-$  respectively residing in the structural channel sites of beryl crystals. On irradiation, these ions lose an electron and become  $\text{CO}_3^{\cdot-}$  and  $\text{NO}_3$  radicals. This results in generation of a hole centre in Maxixe type beryls. Nassau *et al.* (1978) defined *Maxixe beryls* as those natural deep blue beryls formed by natural radiation in which the impurity precursor is  $\text{NO}_3^-$ , whereas *Maxixe type beryls* are those deep blue-green beryls produced by artificial irradiation having impurity precursor as  $\text{CO}_3^{2-}$ . Edgar and Vance (1977) considered, the presence of  $\text{HCO}_3^-$  precursors to be more reasonable than  $\text{CO}_3^{2-}$  due to the formation of neutral hydrogen atom ( $\text{H}^0$ ) after irradiation. In the present study by the author, as discussed earlier, the formation of atomic hydrogen is seen both in the case of electron beam and gamma - ray irradiation; however, no colour is produced from gamma - ray irradiation. This indicates that atomic hydrogen produced from irradiation comes solely from  $\text{H}_2\text{O}$ , and therefore involvement of  $\text{HCO}_3^-$  does not arise in the samples under study.

#### 6.4.4 HEATING EXPERIMENTS (IN AIR)

As discussed earlier, after heating the irradiated beryl to 300 °C, the greenish yellow coloured beryl turned yellow, but no significant change in hue of yellow orange beryl was observed. On heating under controlled conditions to 400 °C, the irradiated greenish yellow colour of sample turns blue. Further heating to 500 °C both greenish

yellow and yellow orange beryl became colourless. The following changes in the optical spectrum were seen *after heating the beryl crystals to 300 °C* (Figures 6.16a and 6.17)

- 1) sharp absorption peaks at 644 and 688 nm which are polarised only along the ordinary ray disappeared
- 2) the intensity of 820 nm band (*o* - ray) decreased
- 3) the intensity of 760 and 920 nm bands (*e* - ray) decreased and
- 4) absorption band at 680 nm (*e* - ray) disappeared

*Further heating to 400 °C, it was observed;*

- 5) 820 nm band (*o* -ray) increased
- 6) the 760 and 820 nm becomes broader with increase intensity and shift towards visible region (650 nm) along (*e* - ray)
- 7) the UVCT tail receded to shorter wavelengths and became steeper.

*On further heating to 500 °C, it was observed that;*

- 8) the intensity of 820 nm band (*o* - ray) further increased
- 9) 650 shift to 820 nm with increase in intensity (*e* - ray).

The first observation indicates that the sharp absorption features at 644 and 688 nm have thermal decay characteristics, which are similar to the observations of Serway (1967) on irradiated calcite. In irradiated calcite, the 650 nm band shows thermal decay behaviour similar to those of the ESR signal attributed to the  $\text{CO}_3^-$  molecular ion. Identical decay characteristics of a narrow absorption band were also observed by Nassau *et al.* (1976) in Maxixe type blue and green beryls (Figure 6.16b). It appears that a defect centre, similar to Maxixe type, probably results in the blue coloration in irradiated Indian

colourless beryl. On heating to 300 °C, the defect centre decays and the crystal becomes yellow

The second and third observations indicate that the amount of  $\text{Fe}^{2+}$  ions residing in the channel as well as in the octahedral sites decrease. These changes are due to the fact that, on annealing, the  $\text{Fe}^{2+}$  in both channel and octahedral sites are converted into  $\text{Fe}^{3+}$  ions. This explains the decrease in the 820 nm ( $\sigma$  - ray), 760 and 920 nm ( $e$  - ray) bands. The above observation indicates that on irradiation there is partial reduction of  $\text{Fe}^{3+}$  to  $\text{Fe}^{2+}$ . A similar feature was also observed by Goldman *et al.* (1978) in a natural yellow beryl sample, which on irradiation and subsequent heating to 500 °C showed recovery of the  $\text{Fe}^{2+}$  ion in the channel as well as in the octahedral site. The complete disappearance of IVCT at 684 nm in the fourth observation is in accordance with the disappearance of  $\text{Fe}^{3+}$  ESR line at 1500 gauss at 300 °C. Thus in addition to the blue colouration due to a Maxixe centre, the IVCT band at 684 nm possibly also contributes to the blue colour after irradiation of colourless beryl.

The fifth observation elucidates increase in concentration of  $\text{Fe}^{2+}$  ion in channel site, while the sixth observation of broadening with increase in intensity of  $\text{Fe}^{2+}$  band at octahedral Al site and shift towards visible region indicates of intervalence charge transfer due to the oxidation-reduction phenomenon, which again gives blue hue in beryl (*Plate 6.2a*). It was observed by the author that if the sample of irradiated beryl is heated rapidly from 300 °C to 400 °C, transforms directly to colourless shade from yellow hue. The fifth and sixth observation are complimented by the seventh observation. This is consistent with the decrease in  $\text{Fe}^{3+}$  concentration accompanied by a recession of the  $\text{Fe}^{3+} - \text{O}^{2-}$  charge transfer band towards ultraviolet region. These changes are accompanied by a change in colour of the sample from yellow to colourless. The eighth observation indicates that the amount of channel  $\text{Fe}^{2+}$  ions has increased on further heating. This suggests that the  $\text{Fe}^{3+}$

ions residing in the channel is reduced to  $\text{Fe}^{2+}$  by the thermal release of electrons. The ninth observation discerns that on heating above 400 °C, the  $\text{Fe}^{2+}$  ion (820 and 920 nm, *e* - ray) is also further increased in concentration at octahedral Al sites due to partial reduction of the  $\text{Fe}^{3+}$  ion to  $\text{Fe}^{2+}$  ion. The IVCT band gets destroyed due to reduction of  $\text{Fe}^{3+}$  ions to  $\text{Fe}^{2+}$ , thereby not facilitating charge transfer to occur and render sample colourless again. It is observed that the major portion of increase in intensity of 820 nm band (*o* - ray), 760 and 920 nm band (*e* - ray) are manifested mainly after 300°C and UVCT tail recession also starts after 300 °C. Therefore it would not be appropriate to correlate the yellow colour formed after irradiation to the UVCT tail arising from  $\text{Fe}^{3+}$  in the channel site.

*Thus the aim of obtaining blue colour from uncoloured beryl using irradiation - heating technique is achieved at 400 °C.*

#### 6.4.5 YELLOW/GOLDEN BERYL (HELIODOR)

Optical spectra of Orissan unheated yellow beryl (*Figure 6.18a & b*) is characterised by broad absorption edge from 390 to 550 nm, which results in a yellow colour, when this absorption edge is present alone (Wood and Nassau, 1968). This absorption edge is on account of the Ultraviolet charge transfer (UVCT) between  $\text{Fe}^{3+}$  -  $\text{O}^{2-}$ , resulting in strongest absorption in the violet region extending upto green due to the presence  $\text{Fe}^{3+}$ , similar to the observation made by the author on colourless beryl by the present author. The spectra reveals low concentration of  $\text{Fe}^{2+}$  at the octahedral Al site, characterised by low absorption at 760 nm along *e*-ray.

On heating to 380 - 400 °C, the yellow colour of yellow beryl is seen transformed to pale blue colour in accordance with earlier workers (Wood and Nassau, 1968, Goldman et al 1978, Sinkankas, 1985 etc.) The author, while heating the present sample observed that, the pale blue colour is obtained only on heating at a controlled rate of heating

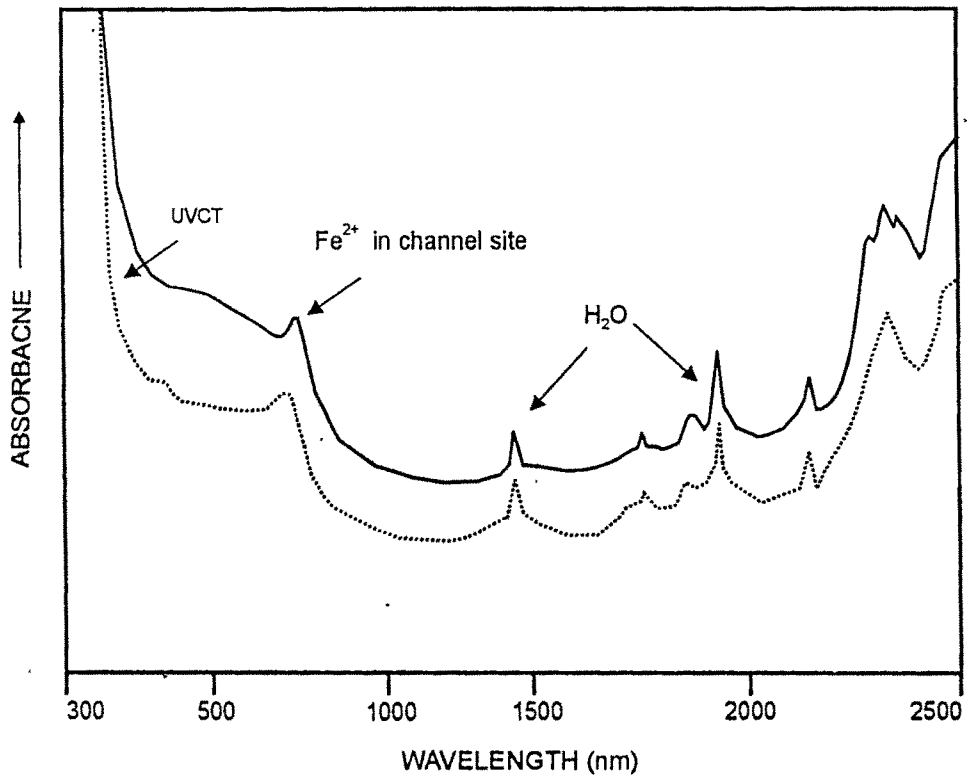


Figure 6.18a : OA spectra of Orissan yellow beryl along o-ray. Room temperature (continous line) and 400°C (dotted line) - turns pale blue

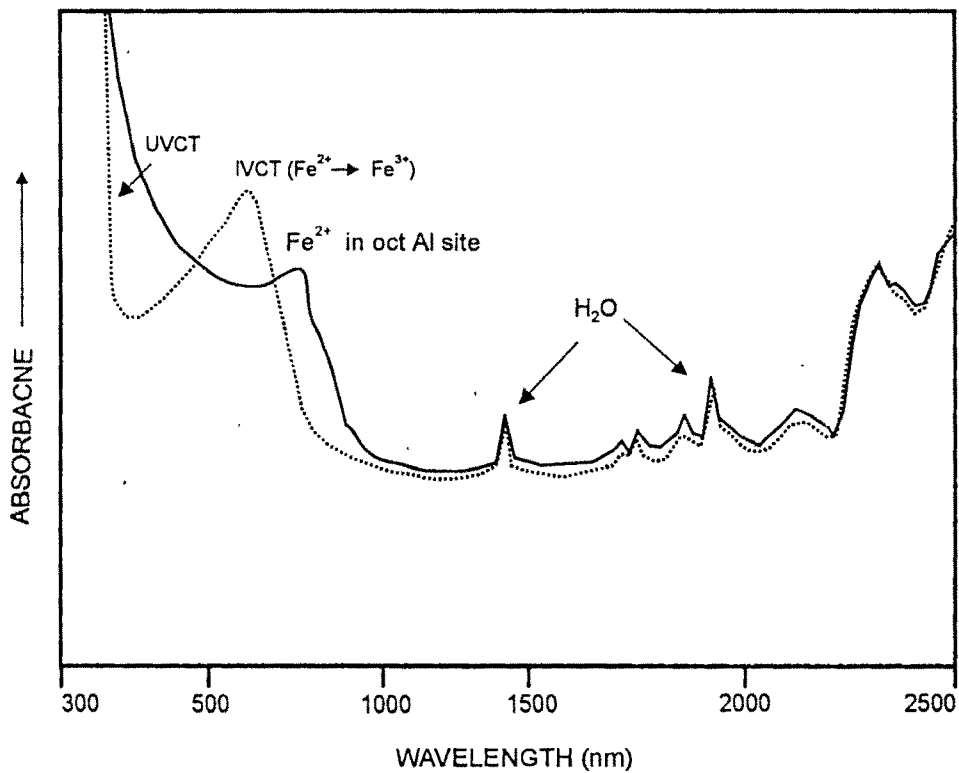


Figure 6.18b : OA spectra of Orissan yellow beryl along e-ray. Room temperature (continous line) and 400°C (dotted line) - turns pale blue

(approx 100 °C in 2hrs). The optical spectra of yellow beryl after heating indicate significant increase in Fe<sup>2+</sup> Crystal field transition band (*e*-ray) as shown in *Figure 6.18b* accompanied by recession of UVCT tail to lower wavelength. Crystal field transition band of Fe<sup>2+</sup> along *o* - ray (*Figure 6.18a*), however, does not reveal any change in intensity except for the shift of UVCT band to lower wavelength. The increase in Fe<sup>2+</sup> absorption band along *e* - ray is consistent with increase in broadness of band accompanied by shoulder around 650 nm. According to Wood and Nassau (1968), broad band near 620 nm observed as shoulder in the *e* - ray spectrum makes beryl blue coloured, but yellow or colourless in the *o* - ray, since 620 nm band removes the red from transmitted light. They opined that it was not due to presence of Fe<sup>2+</sup> in either a six - fold or four - fold site, but is present in channel site. Thus the pale blue colour observed is due to the absorption in the red observed as shoulder at 650 nm.

As the above yellow beryl from Orissa were not of deep coloured ones, a golden yellow (untreated) beryl from Siberia were studied to observe the above said change in colour. The Siberian on heating to 430 - 450 °C changed to deep blue and the optical spectra indicated (*Figure 6.19a & b*) similar features as that of the Orissan one. However, the shoulder along *e* - ray is (*Figure 6.18b*) observed at 700 nm Thus both (light- Orissan and deep - Siberian) yellow beryls on heating to 400 - 450 °C deduce the following :

- 1 . Negligible increase in 820 nm (*o* - ray) band
- 2 . 760 and 920 nm band (*e* - ray) increase in intensity
- 3 . UVCT tail recedes to shorter wavelength.

The first observation elucidates that, the amount of channel Fe<sup>2+</sup> remains unchanged This the author of the thesis attributes due to almost complete absence of Fe<sup>3+</sup> in the channel, so as to get reduced to Fe<sup>2+</sup> on annealing The second observation deciphers that the major proportion of Fe<sup>3+</sup> residing in the Al site gets reduced to Fe<sup>2+</sup>

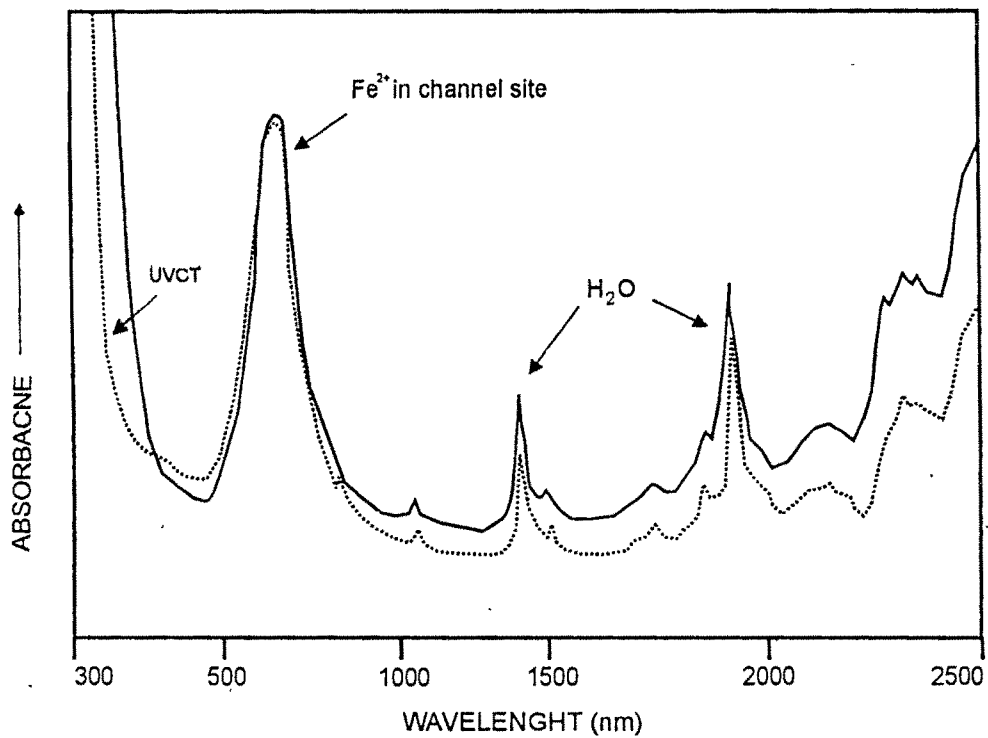


Figure 6.19a : OA spectra of Siberian yellow orange beryl along o - ray. Room temperature (continous line) and 450°C (dotted line)

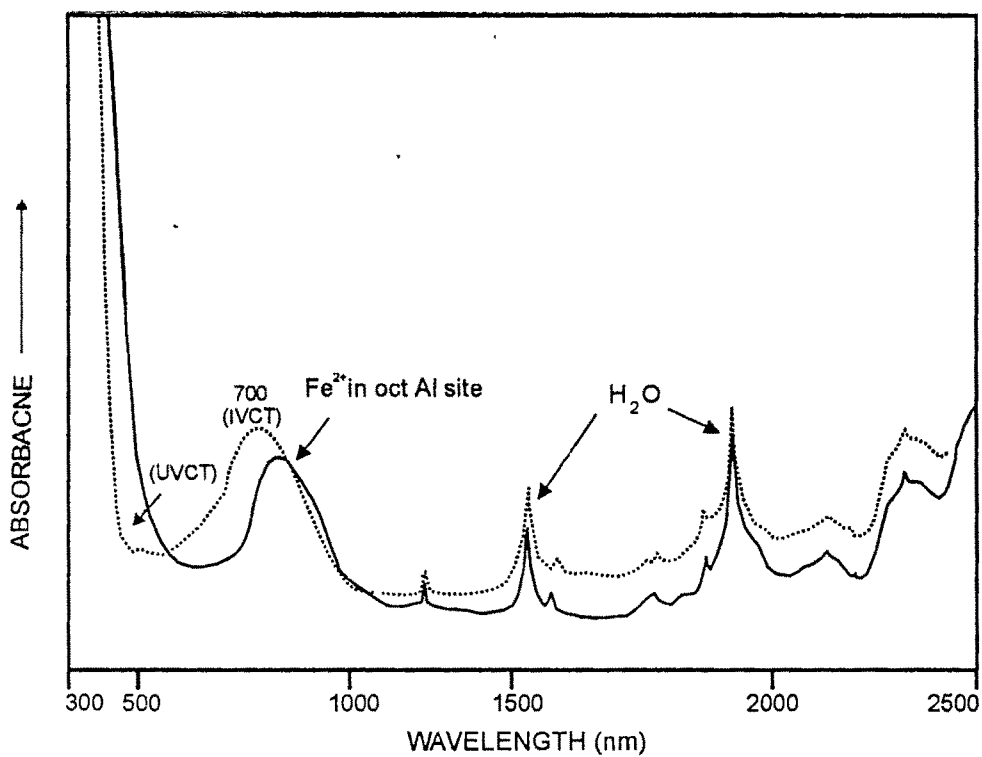


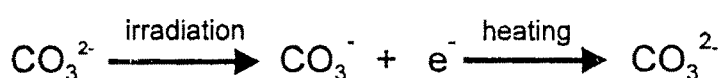
Figure 6.19b : OA spectra of Siberian yellow orange beryl along e - ray. Room temperature (continous line) and 450°C (dotted line)

resulting in an increase of six co-ordinated  $\text{Fe}^{2+}$ . Third observation is consistent with the decrease of  $\text{Fe}^{2+}$  accompanied by shifting of UVCT band to Ultraviolet region. The above changes are accompanied by a change of yellow colour of yellow beryl to blue. Goldman et al (1978) interpreted that the ultraviolet charge transfer tail which is responsible for yellow colour in beryl that arises from  $\text{Fe}^{3+}$  in channel. However, above investigation by the author on yellow beryls corroborates his earlier observation on colourless beryl, that the UVCT tail is on account of  $\text{Fe}^{3+}$  present at octahedral Al site and not from channel. This statement is well evident from *Figures 6.18a & 6.19a*, wherein on heating,  $\text{Fe}^{2+}$  in channel site (820 nm, *o* - ray) indicates absence of increase in concentration characterised by lack of increase in absorption intensity. Whereas  $\text{Fe}^{2+}$  at Al site (760 nm, *e* -ray) shows prominent increase in absorption accompanied by the receding of UVCT tail to higher energy. Thus the author envisages that the UVCT is on account of a charge transfer between  $\text{O}^{2-}$  and  $\text{Fe}^{3+}$  ion present at octahedral Al site.

Goldman et al. (1978) inferred that, 700 nm band neither correlates with amount of channel  $\text{Fe}^{2+}$  nor does it correlate with either the 425 nm or the 372 nm  $\text{Fe}^{3+}$  band. However, it does show a good correlation with the amount of six co-ordinated  $\text{Fe}^{2+}$ . The author attributes 700 nm to  $\text{Fe}^{2+} \rightarrow \text{Fe}^{3+}$  IVCT in accordance with Goldman et al. (1978). The  $\text{Fe}^{2+}$  is substituting aluminium at octahedral site and  $\text{Fe}^{3+}$  is probably occupying the interstitial site, as presence of  $\text{Fe}^{2+}$  in channel site would not favour charge transfer process. This is because the cations here are not occupying adjacent co-ordination site, so that electronic transition assigned to  $\text{Fe}^{2+} + \text{Fe}^{3+} \rightarrow \text{Fe}^{3+} + \text{Fe}^{2+}$  intervalence charge transfer process to occur.

#### 6.4.6 IRRADIATED YELLOW (ORISSAN) BERYL

On irradiation with electron beam, except Siberian all samples yellow of beryls, turned to greenish yellow. The optical spectra reveal similar features as observed for colourless beryl. On heating to 300 °C, the sample again turns to its original hue. This the author attributes to be due to the decay of Maxixe type centre on account of the thermal release of the electron (that had been removed on account of irradiation) trapped somewhere else in the structure by the reaction. It can be expressed by the following equation:



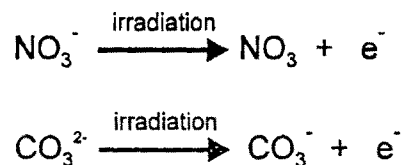
The Siberian beryls did not react to irradiation due to absence of the necessary precursor required for the formation of Maxixe centre and also revealed absence of any IVCT bands

#### 6.4.7 BLUE BERYL (AQUAMARINE)

It can be repeated here that blue beryls in nature are of two types, the one coloured by Fe impurities and other coloured due to the presence of free radicals (colour centre). The colour centre type includes Maxixe and Maxixe type deep blue beryls, almost cobalt blue, about the equal of the colour of sapphire (Nassau, 1994). The latter type that occurs in nature, can also be produced by irradiation. The colour of this type is also not stable; it fades when exposed to light (Nassau, 1973; Nassau and Wood, 1976). The original natural crystal have been found in about 1917 at the Maxixe mine, Brazil (as quoted by Nassau, 1994), but its scientific examinations were published much later. In 1971 similar, but not identical material appeared in the Jewellery trade and has been called Maxixe type beryl

(Nassau and Wood, 1973), It was then stated by Bastos, (1975) that, it can also be produced by a simple process using pink beryl from a mine at Barrade Salinas, Minas Gerais, Brazil.

Detailed examination by Edgar and Vance (1977) and Anderson (1979) indicate that, the blue colour is caused by a colour centre, which can be produced in material containing suitable precursors (Mathew et al. 1998). The precursor was assigned to a nitrate impurity (Anderson, 1979) in the original Maxixe material and a carbonate impurity in more recent Maxixe - type material (Edgar and Vance, 1977; Anderson, 1979). Both of these ions have 24 electrons in their outermost shell and both ( $\text{NO}_3^-$  and  $\text{CO}_3^{2-}$ ) can lose an electron on irradiation to form a 23 - electron resulting in a hole centre.



The aquamarine coloured by Fe impurities and that coloured by Maxixe colour centre are readily distinguished on observing the dichroism while rotating the specimen above a polariser (Nassau, 1994) By rotating the specimen in a dichroscope or merely using a polariser sheet (*Figure 6.20*), the pleochroism can be determined. *o* - ray absorbs darker colour Maxixe and Maxixe type beryl, while in natural aquamarine whose blue colour is due to iron impurity, *e* - ray absorbs deeper colour.

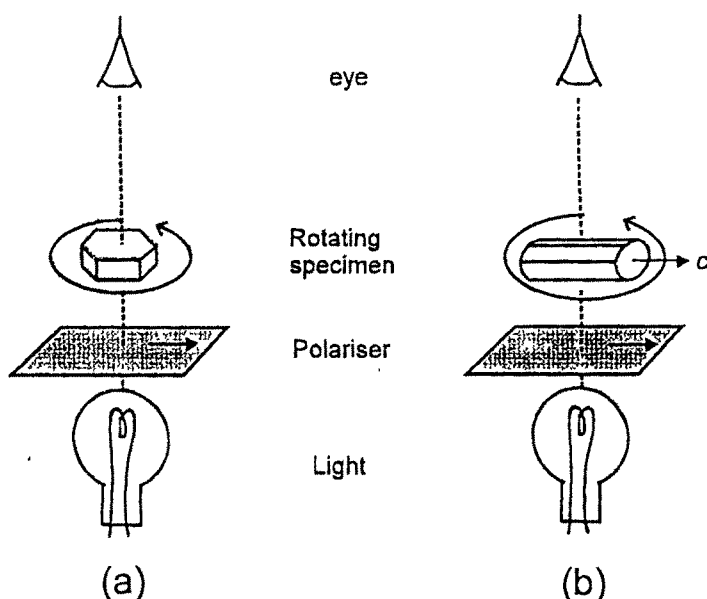


**Figure 6.20 : Distinguishing between aquamarine and the Maxixe beryls by observing the dichroism while rotating the specimen above a polariser. (a) rotation about the optic axis and (b) rotation perpendicular to the optic axis (after Nassau, 1994).**

The optical spectra of blue beryl from Badmal province (*Figure 6.21a*), depicts prominent  $\text{Fe}^{2+}$  crystal field transition in channel site along  $o$  - ray at 808 nm. Crystal transition due to  $\text{Fe}^{2+}$  in octahedral Al site along  $e$  - ray (*Figure 6.21b*) is observed at 820 nm with absorption shoulder around 690 - 700 nm. As discussed earlier in the section on yellow beryl, the shoulder around 620 nm and around 700 nm is considered as the cause for blue colour in beryl by Wood and Nassau, (1968) and later by Goldman et al. (1978). They look blue in the  $e$  - ray and colourless or yellow in the  $o$  - ray because the above band remove red transmitted light (Wood and Nassau, 1968). The author attributes the 700 nm shoulder to IVCT charge transfer as envisaged earlier for yellow to blue colour transformation in yellow beryl.

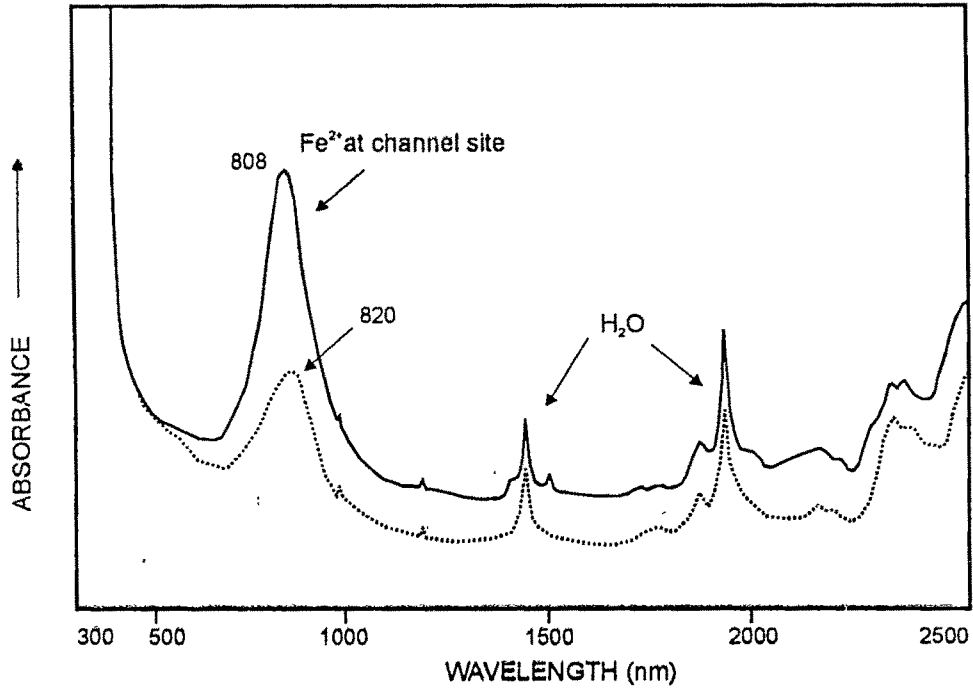


Figure 6.21a : OA spectra of Orissan blue beryl along o - ray. Room temperature(continous line) and 500°C (dotted line)

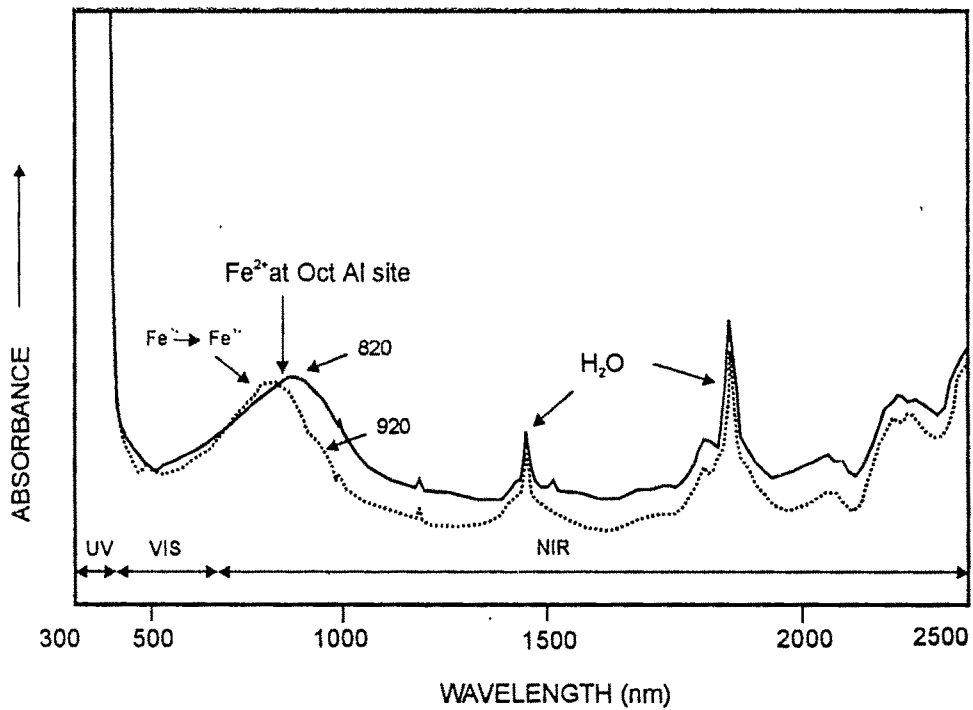


Figure 6.21b : OA spectra of Orissan blue beryl along e - ray. Room temperature(continous line) and 500°C (dotted line)

#### 6.4.8 HEATING EXPERIMENTS (IN AIR)

On heating to 500 °C, the Orissan blue beryls fade to pale blue colour. Optical absorption spectra as shown in *Figure 6.21a*, along *o* - ray it indicates a significant decrease in intensity of 800 nm attributed to channel Fe<sup>2+</sup> ion, whereas intensity of Fe<sup>2+</sup> band at Al site along *e* - ray shifts from 820 to 768 nm without any decrease in intensity of absorption. The decrease in intensity of channel Fe<sup>2+</sup> (*o* -ray) is due to the decrease in concentration of Fe<sup>2+</sup> ion. The decrease is probably due to the oxidation of Fe<sup>2+</sup> to Fe<sup>3+</sup> by the reaction on heating.



However, decrease in intensity of channel Fe<sup>2+</sup> is not accompanied any change in spectra along both ordinary and extraordinary ray (*Figures 6.21 a & b*). This behaviour of Fe<sup>2+</sup> ion in channel site the author presumes to be an independent behaviour and is not related to the fading of colour. The colour fade is probably due to the reduction of interstitial Fe<sup>3+</sup> ion to Fe<sup>2+</sup>, which results in no favourable charge transfer between Fe<sup>2+</sup> at Al site and an interstitial Fe<sup>3+</sup> ion.

In the preceding observations by the author on colourless and yellow beryl, on heating, the Fe<sup>2+</sup> ions either remain unchanged or increase in intensity. The thermal energy (heating) helps in release of electrons trapped somewhere in the structure or by H<sup>+</sup> or alkali ions. The present behaviour of channel Fe<sup>2+</sup> thus warrants detailed investigation as to what mechanism triggers such oxidation to occur.

OAS studies on deep blue beryl from *Karur* (T N.) (*Figure 6.22 a & b*) also reveal similar features as that of Orissan ones. The sample was heated to 600 °C, showed no change in its hue. The spectra at this temperature indicated increase in Fe<sup>2+</sup> intensity along

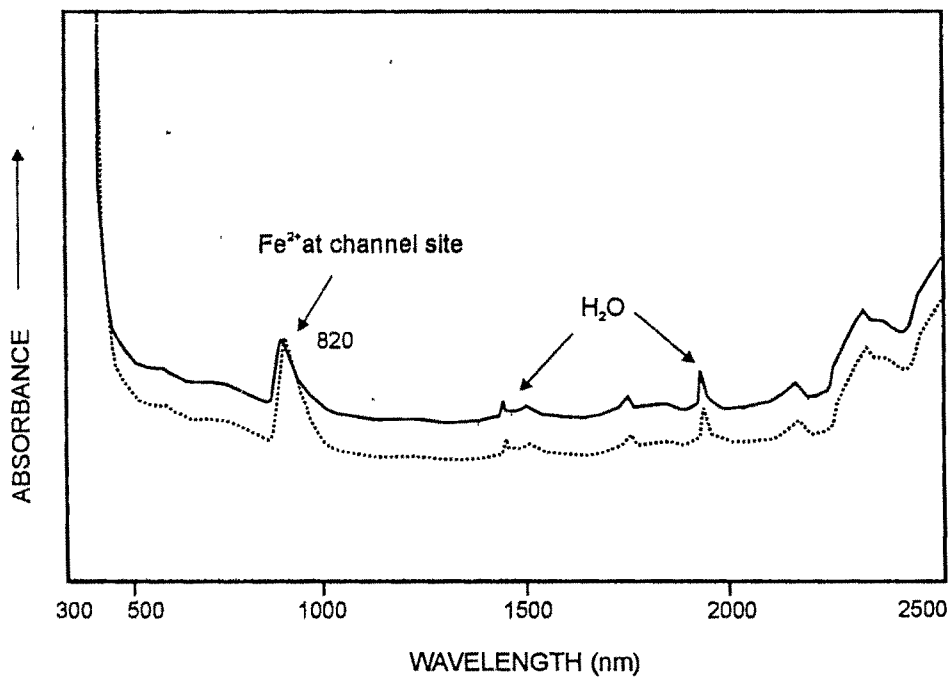


Figure 6. 22a : OA spectra of Tamil Nadu blue beryl along o - ray. Room temperature (continous line) and 600°C (dotted line)

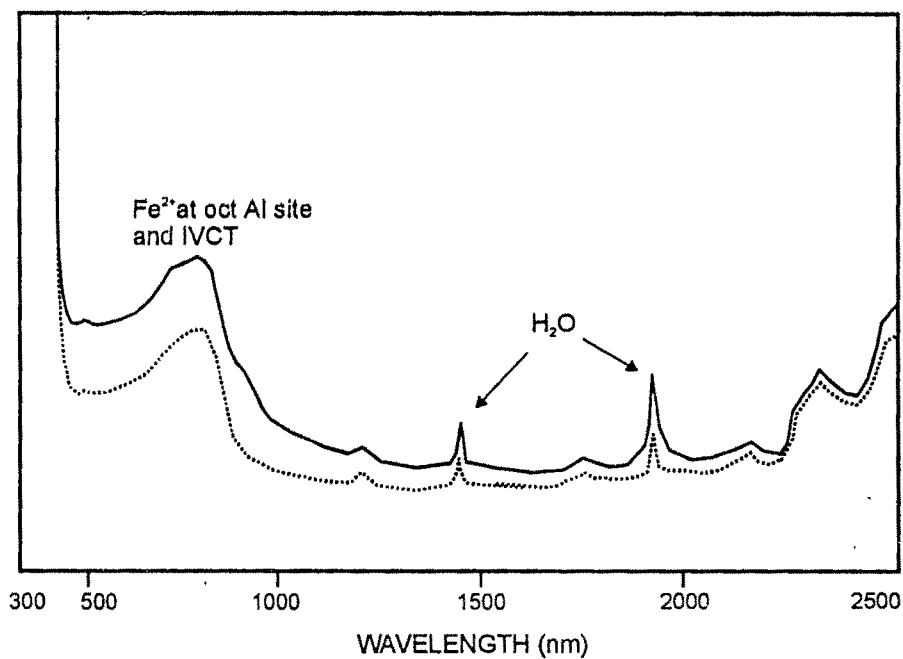
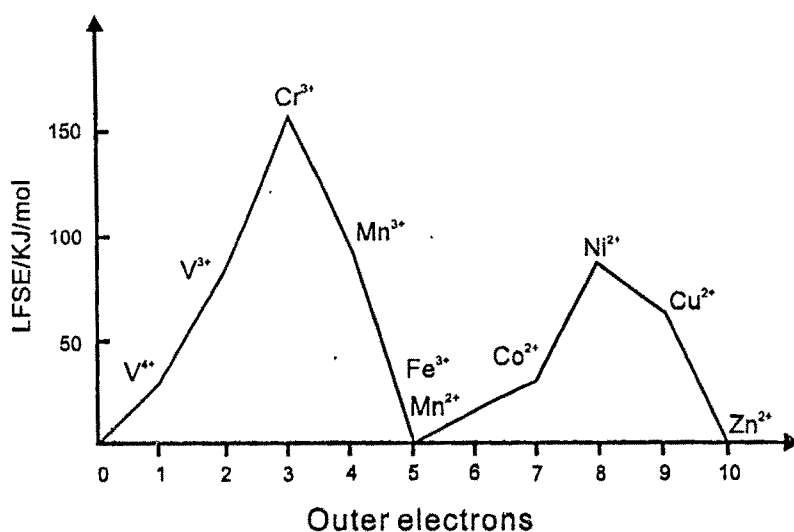


Figure 6.22b : OA spectra of Tamil Nadu blue beryl along e - ray. Room temperature (continous line) and 600°C (dotted line)

$\alpha$  - ray and no observable change along  $e$  - ray. The sample was then further heated to 900 - 1000 °C for bleaching, however, the sample developed innumerable cracks and therefore no further optical spectral studies was possible

#### 6.4.9 GREEN BERYL

Green beryl also includes two types; the one coloured by Cr or V impurities called as 'emerald' and the one most commonly found in nature is coloured by Fe impurities. Beryl containing upto 1.0% of Cr renders a strong green colour (Nassau, 1965). The chromium spectrum in beryl is characterised by two broad bands near 430 and 600 nm and sharp lines at low temperatures; one at blue 476 and two in the red at 680 and 683 nm (Wood and Nassau, 1968). The chromium replace the octahedrally co-ordinated Al ions and this substitution occur with no charge discrepancy ( $\text{Al}^{3+} \leftrightarrow \text{Cr}^{3+}$ ) and with little misfit ( $\text{Al}^{3+} = 0.54 \text{ \AA}$ ,  $\text{Cr}^{3+} = 0.63 \text{ \AA}$ ). Although  $\text{Fe}^{3+}$  ( $0.64 \text{ \AA}$ ) has almost similar ionic radius as  $\text{Cr}^{3+}$ , is also found to substitute other than Al site (e.g.  $\text{Be}^{2+}$  site) as envisaged by the author in the section on colourless beryl. The reason for such kind of substitution with Cr ion always preferring an octahedral symmetry is largely due to site preference energy (or *ligand field stabilisation energy* ( $\Delta$ ) LFSE). The LFSE of  $\text{Cr}^{3+}$  is so large, as shown in *Figure 6.23*, that it can substitute only in sites of octahedral symmetry (Vassilikou - Dova, 1993) and thus achieves high stability and therefore, not affected by irradiation or heating. The absence of any site preference energy for the isoelectronic  $d^5$  ions ( $\text{Mn}^{2+}$  and  $\text{Fe}^{3+}$ ) in six fold or four fold co-ordination sites suggests, that the substitution of them is affected by other factors (Vassilikou - Dova, 1993)



**Figure 6.23 :** Site preference energy for octahedral co-ordination of transition metal  $d^n$  ions with oxygen as ligands (after Vassilikou -Dova, 1993)

In what is referred to as *green beryl*, the green hue is a combination of blue component produced by IVCT and yellow component, a resultant of  $Fe^{3+}$ . Thus emerald is distinctly different from green beryl

*Figure 6.24*, represents unpolarised spectra of light green (Fe bearing) beryl from Orissa. It presents a broad band at 800 nm and ultraviolet charge transfer tail extending into visible region. Thus it well evident that the green colour is due to the UVCT resulting into yellow colour and the broad absorption in the near IR region resulting in blue colour. A combination above two colours thus result in the greenish hue in beryl crystal.

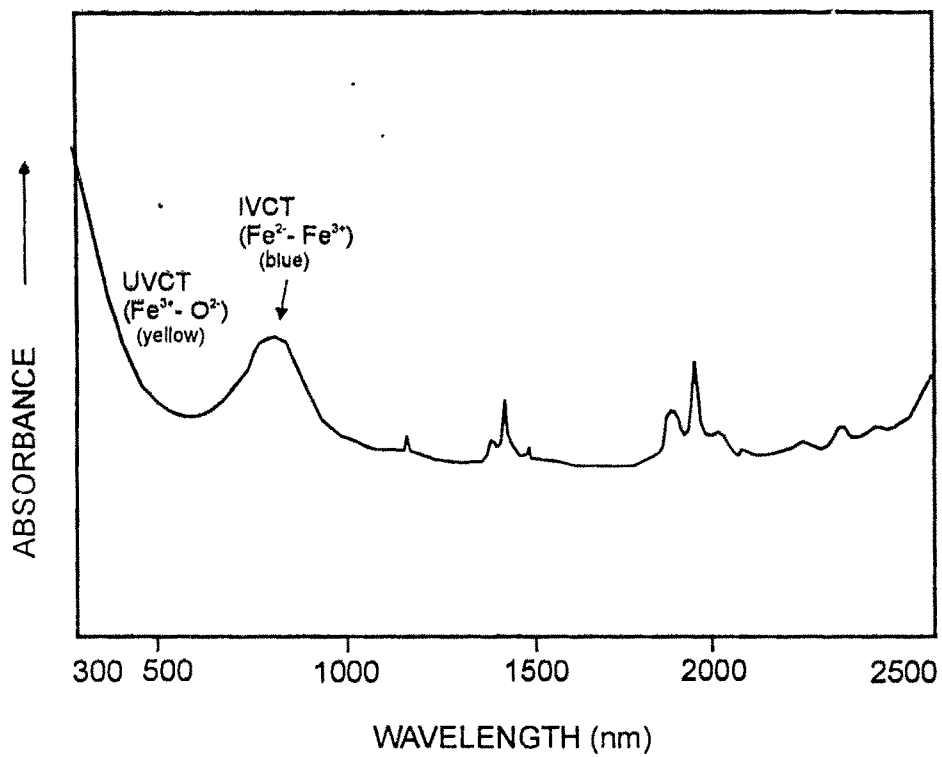


*Figure 6. 24* : Unpolarised optical absorption spectra of green beryl indicating presence of both UVCT and IVCT bands resulting in greenish shade in beryl.

## 6.5 MÖSSBAUER SPECTROSCOPY

Mössbauer spectroscopy is a technique applicable virtually only to solid materials, yielding information about the environment of particular type of nuclei in a solid. This spectroscopy involves emission and absorption of  $\gamma$ -radiation by specific nuclei. The emission of  $\gamma$ -radiation energy from an excited state of nucleus is associated with its decay to the ground state of the same isotope. If a solid sample containing this particular isotope in the ground state is irradiated with  $\gamma$ -rays of the same energy,  $\gamma$ -rays may be absorbed and the nucleus is raised to the excited state. By matching the energy of the incident  $\gamma$ -rays to the exact energy level difference for the specific nucleus absorption will take place.

Since  $\gamma$ -rays have high energy, their emission and absorption is expected to produce recoil in the nuclear mass itself. However, in solid recoil energy is taken up by the vibrational modes in entire crystal. Thus this "recoilless" absorption is the basis of Mössbauer effect, and hence limits its application to solids. Suitable isotopes useful for Mössbauer spectroscopy includes  $^{57}\text{Fe}$ ,  $^{119}\text{Sn}$ ,  $^{121}\text{Sb}$  and  $^{197}\text{Au}$ ; but by far most of the work has been done with  $^{57}\text{Fe}$ .

For a Mössbauer experiment, source for  $\gamma$ -rays should have the same energy as the nucleus in the sample and their source must contain the same isotope as that in the sample and further the isotope in the source must itself be in an excited state. To produce  $^{57}\text{Fe}$   $\gamma$ -radiation, the source used is  $^{57}\text{Co}$  which decays with a half life of 270 days to the excited state of  $^{57}\text{Fe}$ . This excited state then decays emitting the characteristic  $\gamma$ -rays used to probe  $^{57}\text{Fe}$  in the sample. The decay scheme is shown below in *Figure 6.25*.

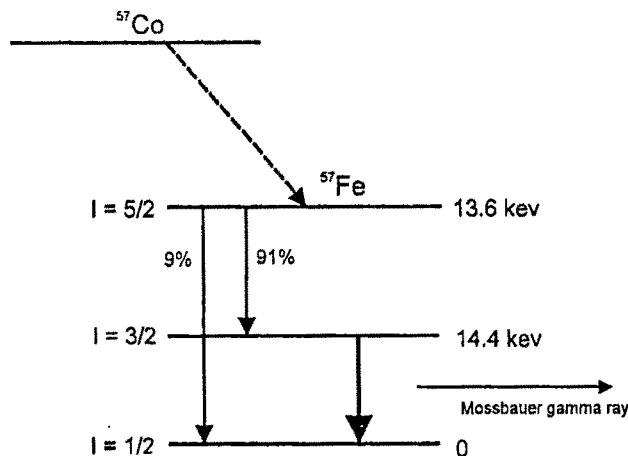


**Figure 6.25 :** Radioactive decay scheme of  $^{57}\text{Co}$  to an excited state of  $^{57}\text{Fe}$ . The relaxation of  $^{57}\text{Fe}$  from this excited state to the ground state involves emission of various  $\gamma$ -rays. The  $3/2$  to  $1/2$  transition emits the 14.4keV  $\gamma$ -rays which are used in the  $^{57}\text{Fe}$  Mössbauer spectroscopy (after Hawthorne, 1988).

The raw data of a Mössbauer spectrum are thus the relative number of  $\gamma$ -rays detected after passing through the sample, as a function of the velocity of the source.

Mössbauer spectra is interpreted based on basically two important parameters:

1. *Isomer or chemical shift* : It is the electric monopole interaction arising from the interaction between positive nuclear charge and the electric field of the surrounding electrons. If the nucleus in the source and the nucleus in the sample have the same environment, transition energy in each will be the same, and mössbauer absorption will take place when the source is stationary with respect to the sample (Figure 6.26a). If the electron density at the nucleus in the source material is different from that in the sample, the mössbauer transition energy will now be slightly different in the two materials. This will appear as a shift in the position of the absorption (Figure 6.26b). The shift is known as chemical shift or Isomer shift. The electron density is principally dependent on the distribution of the 's' valence electrons. The isomer shift is therefore sensitive to any factor that affects the number and distribution of the

valence electrons, which is thus a probe of oxidation state, co-ordination and degree of covalency. In practice, isomer shifts are quoted as ' $\delta$ ' values relative to some standard material.

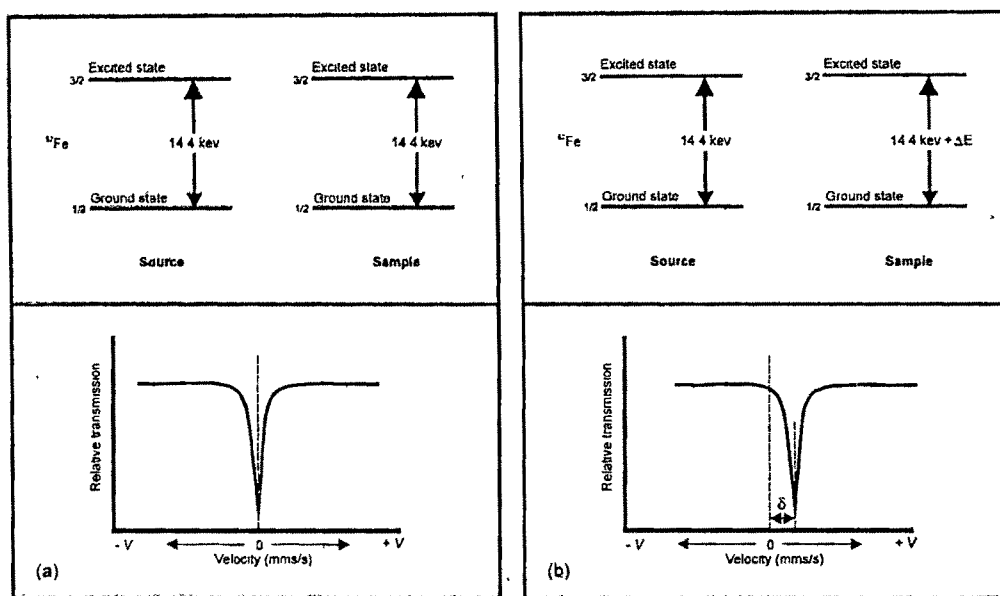


**Figure 6.26 :** a) Mössbauer resonance when the  $^{57}\text{Fe}$  in the source has the same ground state and excite energy as the  $^{57}\text{Fe}$  in the sample, b) Mössbauer resonance when the sample has slightly higher energy difference between ground and excited state than the  $^{57}\text{Fe}$  in the source (after Putnis, 1992).

2. *Quadrupole splitting (Q.S)*: This is electron quadrupole interaction arising from the interaction between the nucleus quadrupole moment and the electric field in which it occurs. When the nuclear spin quantum number  $I > 1$ , the nucleus has a quadrupole moment which may interact with any non - cubic component of the electric field, this leads to splitting of the nuclear energy levels called quadrupole splitting

The above discussion is illustrated using the case  $^{57}\text{Fe}$ . The ground state has spin  $I=\pm 1/2$ , while excited state 14.4 keV higher in energy has a spin  $I=\pm 3/2$ . The presence of an electric field gradient does not affect the ground state, but splits the excited state into  $I=\pm 3/2$  and  $I=1/2$  (Figure 6.27). Thus two transitions from ground state are now possible resulting in two lines in the Mössbauer spectrum. Quadrupole splitting is generally denoted as " $\Delta$ ".

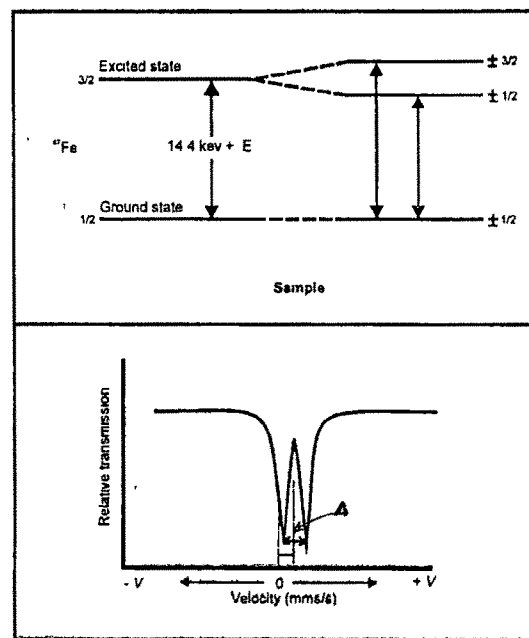


**Figure 6.27 :** Mössbauer resonance when the excited state in the sample is split into two energy levels by the presence of non cubic symmetry in the distribution of electric charge around the nucleus. There are two transitions possible, separated by  $\Delta$  and on either side of the isomer shift position. This is termed as quadrupole doublet (Putnis, 1992).

Mössbauer spectroscopy technique is widely used in mineralogy for a wide range of problems for determination of valency states, oxidation of minerals, electron delocalisation, site occupancy and distortion, magnetic properties etc (Maddock, 1985; Marfunin, 1979b, Bancroft and Burns, 1967)

## EXPERIMENTAL DETAILS

Measurement of the Mössbauer spectra were made on a Mossbauer spectrometer using a  $^{57}\text{Co}$  source in Rhodium source. The spectra were accumulated in 512 channels of a on a multichannel analyser. Calibration was made against the spectrum of iron foil. In addition to ten single crystal prepared as flat plates of 1.5mm thick for mössbauer experiments, two powder samples were also measured. Out of the ten single crystals studied only five samples gave fairly good number of gamma counts so as to be resolved properly. Mössbauer spectra were fitted to component peaks using Normos and Mössfor Mossbauer programme.

### 6.5.1 COLOURLESS BERYL

Mossbauer spectra of the single crystal colourless beryl gave highly scattered gamma absorption counts, whereas powder spectra were found reasonably satisfactory (*Figure 6.28*). The mössbauer of single crystal spectra reveals broad lorentzian line shape near zero velocity and minor ones at low velocity region. Spectral fitting (Hawthorne and Waychunas, 1988) of the spectra discerns three well resolved quadrupole doublets. The fist pair of doublets (I) in *Figures 6.28*, reveals a high quadrupole splitting (Q.S.) value of 2.55 mm/sec and second (II) shows smaller Q.S. 1.06 mm/sec. The third (III, in *Figure 6.26*) closely spaced doublets show very low Q.S. of 0.34 mm/sec. The isomer or chemical shift ( $\delta$ ) compared with the iron foil indicates the first (I) doublet with  $\delta = 1.23$  mm/sec and the second doublet (II) with  $\delta = 1.12$  mm/sec. Such high isomer shifts are characteristic of  $\text{Fe}^{2+}$  ions (Maddock, 1985; Bancroft et al., 1967). Isomer shift of 0.01 mm/sec revealed by the third (III) doublet (*Figure 6.28*) is indicative of the presence of  $\text{Fe}^{3+}$  paramagnetic ion.

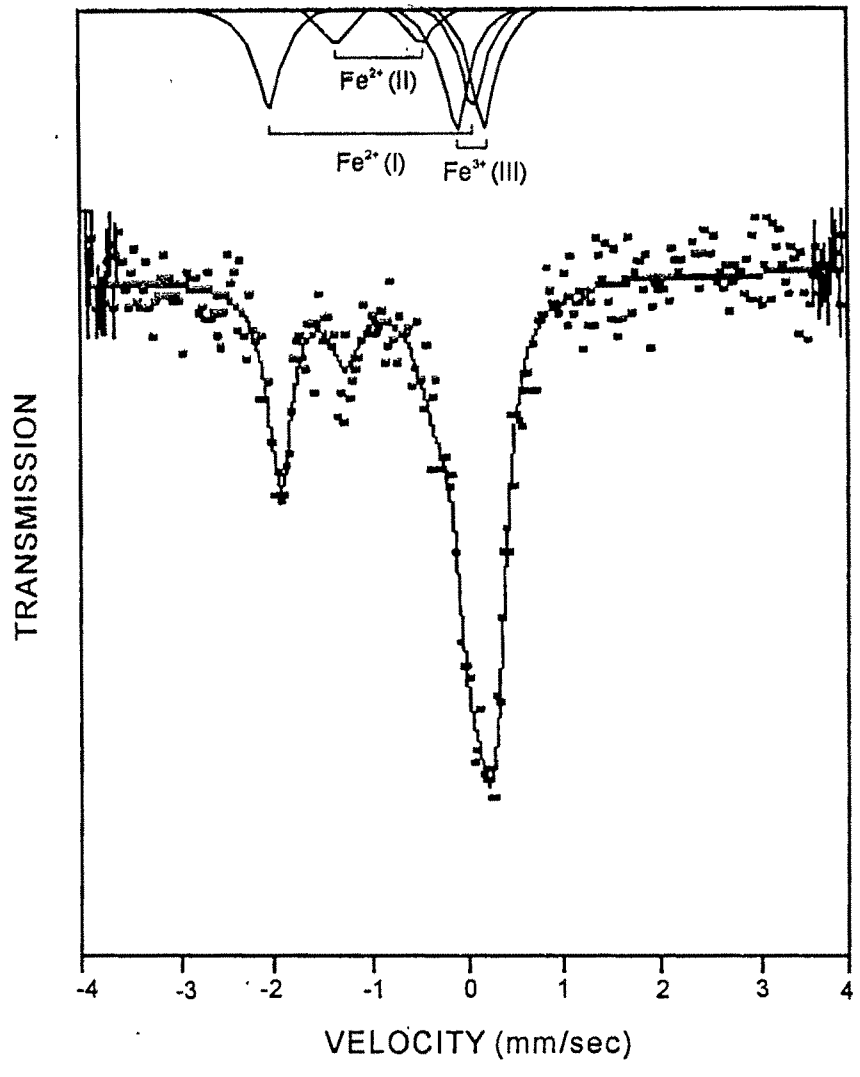


Figure 6.28 : Mössbauer spectra of colourless beryl (powder)

Thus the Mössbauer spectra of colourless beryl deduce presence of two  $\text{Fe}^{2+}$  sites in the beryl lattice. For a six coordinated  $\text{Fe}^{2+}$  species the chemical shift and quadrupole splitting decreases with increasing distortion from octahedral symmetry, whereas for the six coordinated  $\text{Fe}^{3+}$  species, the Q.S splitting becomes larger and the chemical shift is smaller with increasing distortion of near by atoms from octahedral symmetry (Bancroft et al., 1967a; 1967b). Wood and Nassau, (1968) and Goldman et al. (1978) advocated that the majority of Fe ions would prefer either octahedral or channel sites and not tetrahedral Be or Si site.

A perfect undistorted octahedron is expected to show Q.S near to 3.0 mm/sec (Bancroft et al., 1967b). The  $\text{Fe}^{2+}$  doublet with Q.S. = 2.55 mm/sec for the first doublet (I) in the present study indicates, is substituting at Al site. Slight mismatch due to the substitution of  $\text{Fe}^{2+}$  (0.74 Å) and Al (0.54 Å) would thus result in constrain on Al polyhedron and therefore probably gets slightly distorted in the form of axial elongation of polyhedron (Davir and Low, 1960, Gibbs et al., 1968). The Q.S. value of 2.55 mm/sec observed in the present study is analogous to the six coordinate site in corderite, which gives an outer doublet with Q.S. - 2.31 mm/sec (Goldman et al., 1977; Parkin et al., 1977)

The quadrupole and chemical shift for tetrahedral four coordinate  $\text{Fe}^{2+}$  and  $\text{Fe}^{3+}$  is less than for octahedral (Bancroft, 1973; Maddock, 1985, Hawthorne, 1988). In the present study presence of second (II)  $\text{Fe}^{2+}$  doublet (*Figure 6.28*) with Q.S. value of 1.06 mm/sec deduce presence of  $\text{Fe}^{2+}$  ions either tetrahedral or channel site. Presence of  $\text{Fe}^{2+}$  in channel site is not expected to show high Q.S., as in the channel site these ions are weakly bonded to the oxygen of surrounding silicate ring. Moreover, large diameter of the channel (2.8 and 5.1 Å) further do not support for strong bonding. However, since the  $\text{Fe}^{2+}$  ions are held tightly in the channel by the water molecules, they are expected to show fairly high Q.S. than that of  $\text{Fe}^{3+}$  at the same site (Prof. D R.S Sommayajulu, personal. Comm.).

Therefore, the author attributes the second doublet of  $\text{Fe}^{2+}$  to channel site. Presence of  $\text{Fe}^{2+}$  at tetrahedral site probably is unresolved due to its presence in small concentration at this site, but are discerned in the ESR spectra (*Figure 6.7*) as discussed earlier.

Presence of intense  $\text{Fe}^{3+}$  doublet with low Q.S of 0.34 mm/sec indicates that they are probably arising from the channel site. Moreover, such intense (30%, *Table 6.3*)  $\text{Fe}^{3+}$  band at substitutional octahedral site would result in yellow hue in beryl in accordance with other workers (Wood and Nassau, 1968; Samolovich et al., 1971). The low half width (0.30 mm/sec, *Table 6.3*) of this  $\text{Fe}^{3+}$  peak provides further evidence that it is occupying a single site in colourless beryl crystal. thus the above Mössbauer spectra of colourless beryl corroborates the author conclusion from ESR and OA studies that although colourless beryl contains appreciable paramagnetic ions, but are not present at the colour causing sites.

### 6.5.2 BLUE BERYL

Mossbauer spectral features of blue beryl powder sample reveals presence of two  $\text{Fe}^{2+}$  doublets with Q.S of 2.32 mm/sec and 1.87 mm/sec. No resolvable  $\text{Fe}^{3+}$  bands were observed. Its presence, however, were discerned in single crystal experiment (*Figure 6.29*) Mossbauer spectra of single crystal blue beryl indicates an intense and a minor peak high velocity region, while low velocity region reveals broad absorption band. Spectral fitting reveals presence of three resolvable doublets (*Figure 6.29*). The outer doublet (Q.S. - 2.40 mm/sec) is assigned to  $\text{Fe}^{2+}$  at octahedral Al site, whereas the other  $\text{Fe}^{2+}$  doublet with Q.S. - 0.82 mm/sec arises probably from tetrahedral or channel site.

As discussed earlier, in the channel site the ions are held weakly by Van der Waals bond to the neighbouring oxygen ligands of silicate tetrahedra. Presence of  $\text{Fe}^{2+}$  at highly distorted (Davir and Low, 1960, Gibbs et al., 1968) tetrahedral  $\text{Be}^{2+}$  site is also expected

**Table 6.3 : Summary of various Mössbauer parameters obtained for various coloured beryls from Orissa**

Colour of beryl	Quadrupole splitting ( $\Delta$ )	Isomer shift ( $\delta$ )	Width	Area	Fe <sup>2+</sup> /Fe <sup>3+</sup>	$\chi^2$
Colourless beryl	(I) 2.55	(I) 1.23	0.38	48%	Fe <sup>2+</sup>	1.09
	(II) 1.06	(II) 1.12	0.46	20%	Fe <sup>2+</sup>	
	(III) 0.30	(III) 0.01	0.30	31%	Fe <sup>3+</sup>	
Blue beryl	(I) 2.40	(I) 1.31	0.67	68.9%	Fe <sup>2+</sup>	1.04
	(II) 0.82	(II) 2.07	0.21	22.0%	Fe <sup>2+</sup>	
	(III) 0.55	(III) 0.04	0.31	9.1%	Fe <sup>3+</sup>	
Green beryl	(I) 2.51	(I) 1.21	0.38	33.9%	Fe <sup>2+</sup>	1.09
	(II) 0.87	(II) 2.07	0.19	16.7%	Fe <sup>2+</sup>	
	(III) 0.68	(III) 0.07	0.62	49.4%	Fe <sup>3+</sup>	
Siberian Yellow beryl	(I) 1.71	(I) 1.55	0.40	25.3%	Fe <sup>2+</sup>	1.25
	(II) 1.50	(II) 0.90	0.26	30.4%	Fe <sup>2+</sup>	
	(III) 0.65	(III) 0.15	0.62	44.2%	Fe <sup>3+</sup>	

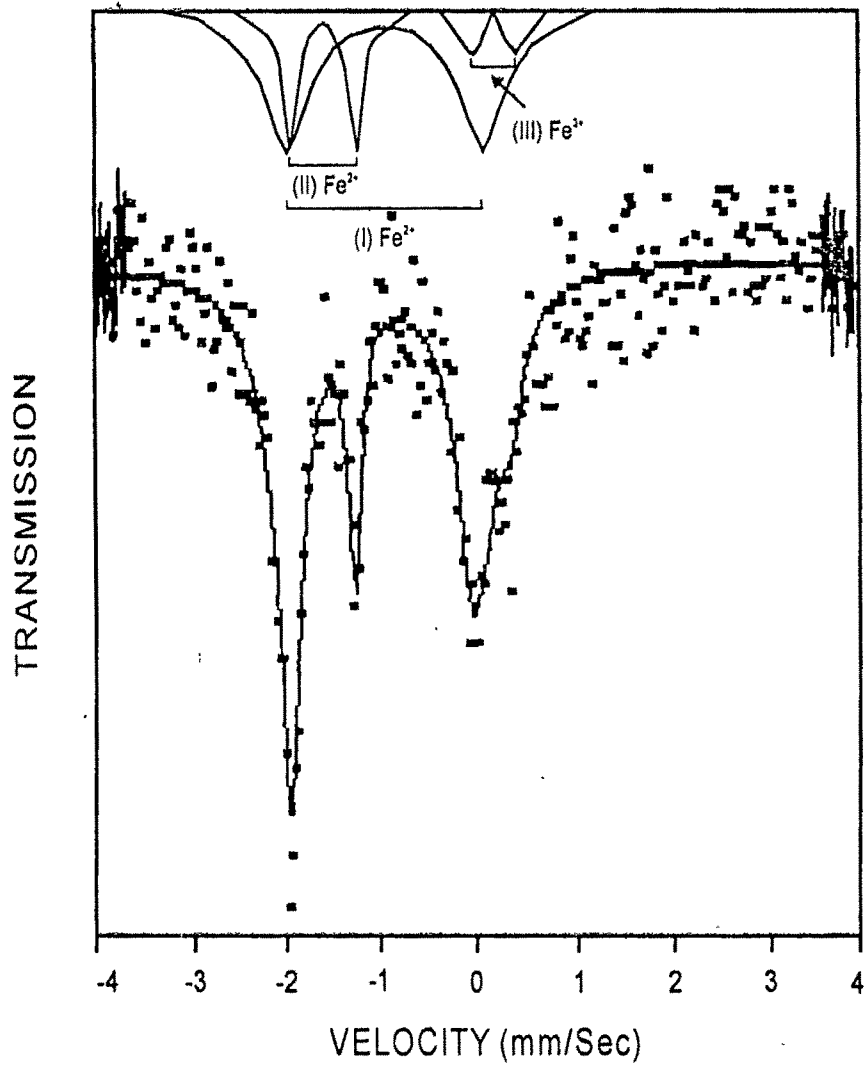


Figure 6.29 : Mossbauer spectra of single crystal blue beryl

to lower the quadrupole splitting value. Therefore, an unambiguous assignment of the second  $\text{Fe}^{2+}$  doublet is difficult.

Presence of minor proportion of  $\text{Fe}^{3+}$  (9%) is evidenced by the presence of third doublet (III) with low Q.S. and isomer shift of 0.55 and 0.04 mm/sec respectively. Higher quadrupole splitting value (0.55 mm/sec) compared to colourless beryl (0.30 mm/sec) indicate that, they are probably substituting at octahedral Al site. Presence of  $\text{Fe}^{3+}$  in channel site is, however, not ruled out since its peak also lies close to the Al site. According to Bancroft (1970) if two peaks are closer than their half widths at half peak height, they cannot be resolved by computer. The broadness of  $\text{Fe}^{3+}$  peak in blue beryl (*Figure 6.29*) is further indicative of presence of  $\text{Fe}^{3+}$  ion in more than one site (Burns and Greaves, 1971). Such information's are unattainable from X-ray crystallography.

Thus mössbauer spectra of blue beryls indicate presence of  $\text{Fe}^{2+}$  and  $\text{Fe}^{3+}$  ion in multisites, thereby facilitating in intervalence charge transfer between  $\text{Fe}^{2+} \rightarrow \text{Fe}^{3+}$  resulting in blue hue

### 6.5.3 GREEN BERYL

Mossbauer spectra of single crystal green beryl (*Figure 6.30*) reveal similar features as that of blue beryl, except for the intense and broad band at higher velocity region. The outer first doublet (I) is attributed to  $\text{Fe}^{2+}$  at octahedral Al site, while the inner one is ascribed to  $\text{Fe}^{2+}$  either tetrahedral or channel site; similar to blue beryl earlier. The most important component of green beryl mössbauer spectra is the presence of  $\text{Fe}^{3+}$  ion (Q.S. - 0.60 mm/sec) occupying almost 50% of the area in the spectra (*Table 6.3*). The much higher quadrupole splitting value in green beryl compared to blue (Q.S. - 0.55 mm/sec) indicates presence of major proportion of  $\text{Fe}^{3+}$  at Al site, while minor proportion

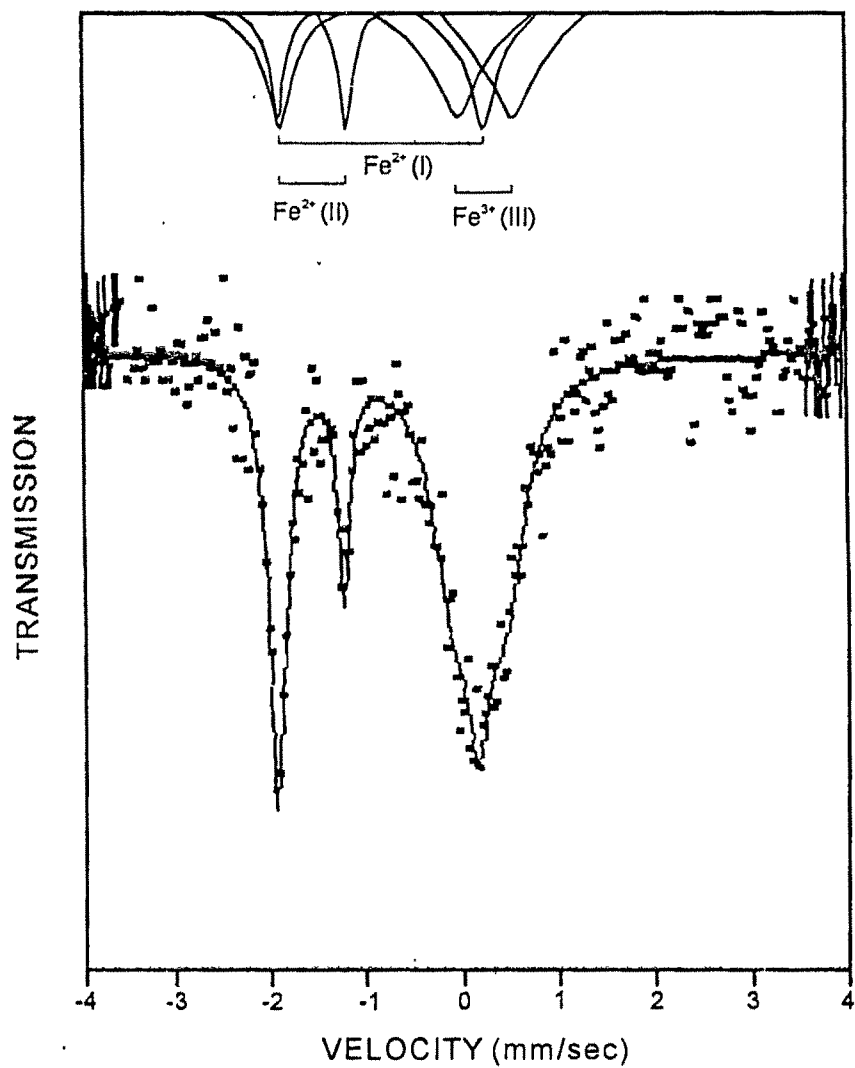


Figure 6.30 : Mossbauer spectra of single crystal green beryl

in channel site. Higher half width (0.62 mm/sec) for  $\text{Fe}^{3+}$  in green beryl also is further indicative of its presence in more than one site.

Presence of higher proportion of  $\text{Fe}^{3+}$  ions would thus result in yellow hue to beryl. This along with the blue hue caused by IVCT results in green shade to beryl crystal.

#### 6.5.4 SIBERIAN YELLOW BERYL

Mössbauer experiments on yellow beryls from Orissa gave highly scattered spectra resulting again poor resolution of various spectra. However, yellow beryls from Siberia revealed fairly good spectra, although cannot be considered satisfactory due to less number of gamma counts absorbed as shown in *Figure 6.31*.

Mössbauer spectra of Siberian yellow beryl (*Figure 6.31*) reveals intense, broad band high velocity region compared to sharp bands at low velocity region. The first two doublet are again attributed to  $\text{Fe}^{2+}$  ions. The high half width (0.62; *Table 6.3*) in this case is again indicative of its presence in more than one site. The presence of only 25% (*Table 6.3*) of  $\text{Fe}^{2+}$  ions in octahedral site is further indicative that the Fe ions at octahedral Al site are in trivalent state. As explained earlier the Mössbauer spectra of yellow beryl under study is of poor quality due to large background scatter. The fitted spectrum also seems unsatisfactory as indicated by high *chi* square value (*Table 6.3*).

*Studies by Parkin et al. (1977), Goldman et al. (1978) Sanders and Doff (1992), revealed just the presence of both bivalent and trivalent iron ions, but they were not able to resolve properly by spectral fitting. The present study by the author is the first detailed Mössbauer studies on beryl crystals. However, due low Fe ion concentration a definite assignment still lacks. Therefore Mössbauer studies using higher source power (>50millicurie) would throw further insight into their possible location in the beryl lattice and their interaction resulting in various shades of colour in beryls.*

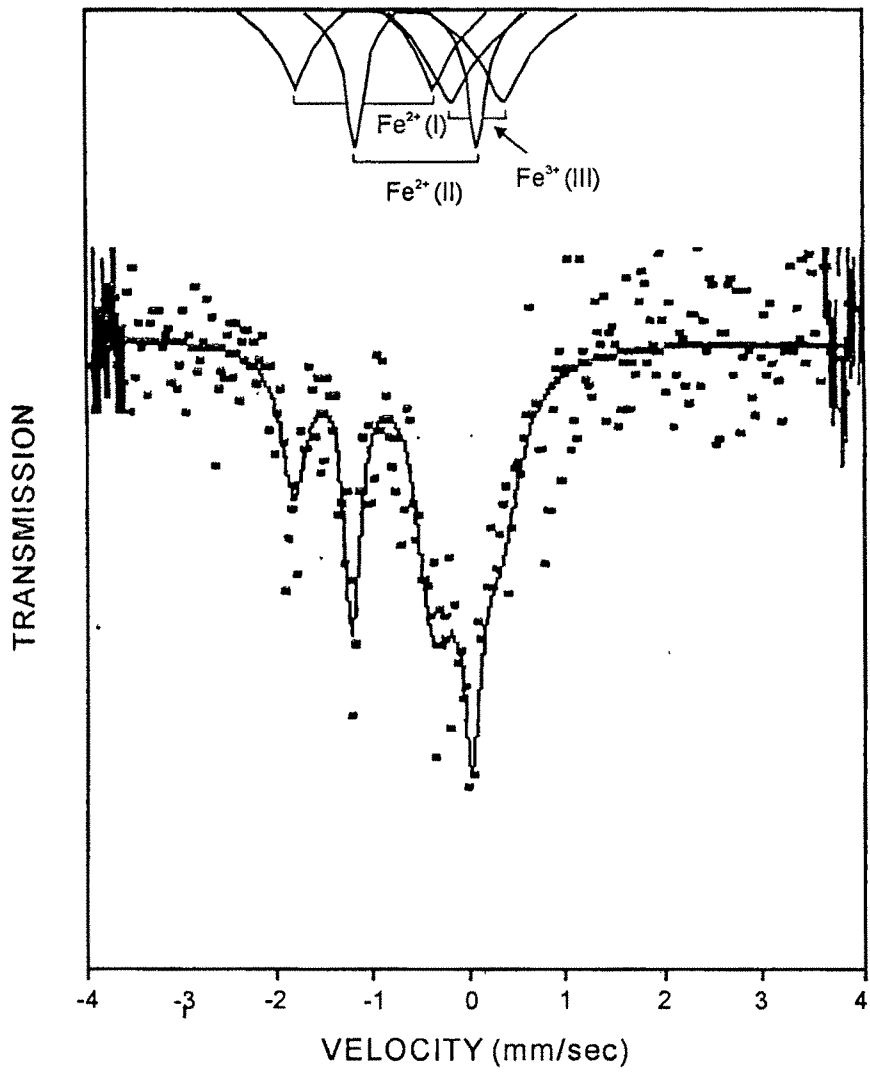


Figure 6.31 : Mossbauer spectra of single crystal Siberian yellow beryl